

Multiple Flows Scheduling in Dense M2M Networks



By

Farhan Nawaz

Fall 2016-MS(EE)-8-00000172493

Supervisor

Dr. Syed Ali Hassan

Department of Electrical Engineering

A thesis submitted in partial fulfillment of the requirements for the degree
of Masters of Science in Electrical Engineering (MS EE)

In

School of Electrical Engineering and Computer Science,
National University of Sciences and Technology (NUST),

Islamabad, Pakistan.

(June 2018)

Approval

It is certified that the contents and form of the thesis entitled “**Multiple Flows Scheduling in Dense M2M Networks**” submitted by **Farhan Nawaz** have been found satisfactory for the requirement of the degree.

Advisor: Dr. Syed Ali Hassan

Signature: _____

Date: _____

Committee Member 1: Dr. Sajid Saleem

Signature: _____

Date: _____

Committee Member 2: Dr. Fahd Ahmed Khan

Signature: _____

Date: _____

Committee Member 3: Dr. Hassaan Khaliq Qureshi

Signature: _____

Date: _____

Abstract

Wireless Sensor Networks (WSNs) have the ability to monitor a specified area with the help of various sensors employing Machine-to-Machine (M2M) communication. These M2M networks have wide areas of applications which include agriculture, structural health monitoring, security and surveillance in buildings, and smart grid systems. The main purpose of having a large number of sensors is to gather the data from one or more of these sensors and to convey the data to a central repository for further processing or necessary actions. In a sensor network, different transmissions take place between multiple source-destination pairs. Each of the pair transmission is associated with a certain schedule. Our focus in this thesis is basically to find the multiple schedules that are being followed in a network. We first perform our analysis on a single hop network, where multiple devices convey their decisions to a far away destination using an orthogonal frequency division multiplexing (OFDM) packet. Taking this work as a starting point, we model a multi-hop linear striped-shaped network where each hop or a level contains a single node and the distance between the nodes is kept constant. This model provides the basis for detecting multiple schedules in a large scale opportunistic large array (OLA) network with multiple nodes in a level. In

this work, an OFDM packet with orthogonal sub-carriers is considered, which travels from the source to the destination. The cooperative devices present in source-destination path poll their schedules in their respective sub-carriers. All the successive transmissions in a linear network are modeled using an irreducible discrete time Markov chain. Three different cases are discussed for detecting a certain schedule. The probability transition matrix for the Markov chain, based on different distributions of the received signal energy is derived, whose left eigen vector gives the probability measure for detecting the schedules.

Dedication

I dedicate this thesis to my father **Mr. Malik Allah Nawaz**, mother **Tehmina Hameed** and my sisters **Afshan Nawaz & Kiran Nawaz** for their endless prayers, love and encouragement.

Certificate of Originality

I hereby declare that this submission is my own work and to the best of my knowledge it contains no materials previously published or written by another person, nor material which to a substantial extent has been accepted for the award of any degree or diploma at NUST SEECS or at any other educational institute, except where due acknowledgement has been made in the thesis. Any contribution made to the research by others, with whom I have worked at NUST SEECS or elsewhere, is explicitly acknowledged in the thesis.

I also declare that the intellectual content of this thesis is the product of my own work, except for the assistance from others in the project's design and conception or in style, presentation and linguistics which has been acknowledged.

Author Name: **Farhan Nawaz**

Signature: _____

Acknowledgment

First of all I would like to thank ALLAH Almighty for HIS blessings on me to carry out this research work. Secondly, I would like to express my sincere and deepest gratitude to my advisor Dr. Syed Ali Hassan for his continuous support, patience, motivation and immense knowledge during the course of my Master studies and related research. He has been a friend and a mentor whose guidance helped me in completing my research and writing of this thesis. Finally, I would like to thank my most supportive, understanding and dedicated parents as without their encouragement and guidance, I would not have been able to achieve what I have thus far.

Table of Contents

1	Introduction	1
1.1	Cooperative Transmissions in OLA Networks	3
1.1.1	Basic OLA	3
1.1.2	OLAPRISE	4
1.1.3	OLAROAD	4
1.2	Need for Duty Cycling in OLA Networks	5
1.3	Introducing Additional Stages in OLAPRISE	5
1.3.1	Polling Query	5
1.3.2	Schedule Assignment	6
1.4	Thesis Motivation	6
1.5	Thesis Contribution	7
1.6	Thesis Organization	7
2	Literature Review	9
3	One Shot Polling of Wireless Sensors	14
3.1	System Model	15
3.2	Statistics of the Received Signals	17

<i>TABLE OF CONTENTS</i>	viii
3.2.1 Non Line-Of-Sight (NLOS) Channel	17
3.2.2 Line-Of-Sight (LOS) Channel	18
3.3 Neyman-Pearson Detection Tests	21
3.3.1 NP Test for the NLOS Channel	21
3.3.2 NP Test for the LOS Channel	23
4 Polling of Sensors in a Multi-hop M2M Network	24
4.1 System Description	24
4.2 Modeling by Markov Chain	29
4.2.1 Strict Approach	29
4.2.2 Lenient Approach	30
4.2.3 Diversity Approach	31
4.3 Formulation of the Transition Probability Matrix	35
4.3.1 Strict Approach	36
4.3.2 Lenient Approach	37
4.3.3 Diversity Approach	37
5 Results and Discussions	39
5.1 Results for One Shot Polling of Wireless Sensors	39
5.2 Results for Polling of Sensors in a Multi-hop M2M Network . .	44
6 Conclusion & Future Works	50

List of Figures

1.1	The key technologies in 5G systems.	2
3.1	(a) An airborne collector receiving the information from the sensors on ground (b). BS receiving the information from a co-located cluster of sensors	15
4.1	The system model showing a new source-destination route crossing two already existing routes.	26
4.2	The OFDM packet with 12 sub-carriers, i.e., $S = 4$ and $K = 3$.	28
4.3	The state space representation of $\mathbb{Y}(l)$ for $S = 4$	32
4.4	The working of Algorithm 1 for $S = 4$, $s = 2$, and $\delta = 4$	35
5.1	The ROC curves for different values of K_1 and K_2 but for same values of S_1 and S_2 , i.e., $S_1 = S_2 = 20$, at 10dB of SNR with NLOS channel	40
5.2	The ROC curves for $K_1 = K_2 = 10$ for varying values of S_1 and S_2 at SNR of 10dB in a NLOS channel.	41
5.3	Contour plot of probability of detection for varying SNR; $K_1 = K_2 = 10$, and $P_{FA} = 0.05$	42

5.4	The error performance vs. the SNR for varying values of K_1 and K_2 ; $S_1 = 5$, and $S_2 = 0$	43
5.5	The ROC curves for both LOS and NLOS channels at $K_1 = 20$, $K_2 = 10$, and $S_1 = S_2 = 200$	43
5.6	The probability of detection for different number of hops for varying P	45
5.7	The probability of detection against the transmit power, P , for varying K	46
5.8	The outage probability vs. the transmit power, P , for varying S	47
5.9	The probability of detection for different combinations of n_1 , n_2 and n_3	48
5.10	The outage probability against different thresholds for $S = 4$	49

List of Tables

3.1	K-S test for CDF approximations.	21
-----	--	----

Chapter 1

Introduction

In the modern era of fifth generation (5G) networks, wireless ad hoc and sensor networks have gained renewed interest in the context of Internet-of-Things (IoT) networks [1–5]. These ad hoc networks generally involve Machine-to-Machine (M2M) communication without the involvement of human beings and operate without any existing infrastructure and are decentralized [6–8]. Since, the devices used in these networks are low cost and battery-limited, therefore, they cannot send messages to far off destinations; an issue known as *reach back problem* in some applications [9]. The information is usually broadcasted among the sensor nodes using some medium access control (MAC) protocol, such as ad hoc on-demand distance vector (AODV) protocol, which causes overhead, low throughput and high latency in the network [10]. Furthermore, wireless networks are under the influence of multi-path fading [11–13], which creates difficulty in reliable communication. Therefore, reliability in such networks is possible only when the nodes work in a cooperative manner.

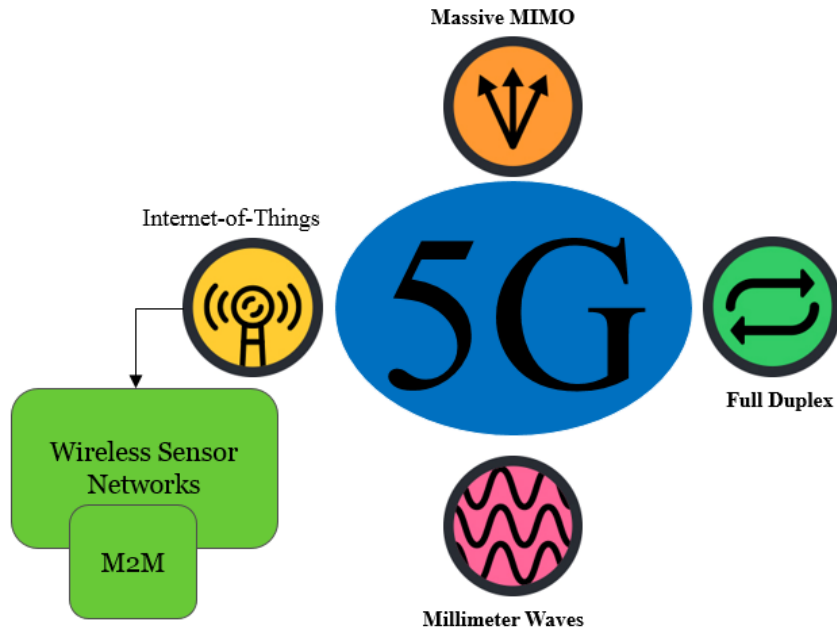


Figure 1.1: The key technologies in 5G systems.

In a cooperative transmission (CT), the intermediate nodes present in a source-destination path act as relays and help in forwarding the source message towards the destination [14]. An immense improvement in the network performance has been achieved through this physical layer technology in many ways, such as, through improvement in bit error rates, reliable transmission and outage probability. It also provides a significant gain in terms of capacity and robustness [15], [16]. Such multi-hop CT networks have gained a lot of importance in the areas of cellular networking, mobile computing, and computer networking, etc.

At the physical layer, a very new and optimistic technique of CT is Opportunistic Large Array (OLA), where the source message travels from one layer of radio nodes to another layer [17]. By using OLA, the complexity of the system increases as the avalanche of the incoming signals produces a

stronger signal at the destination but at the same time, the system vulnerability becomes much lower. OLA can easily be implemented on any network or system and a huge amount of work has been done in the past few years on OLA networks by considering different network topologies [18–20].

1.1 Cooperative Transmissions in OLA Networks

Cooperative transmissions in the large scale OLA networks can be achieved by the following three basic protocols.

1.1.1 Basic OLA

In a basic OLA protocol [21], the source node broadcasts the signal in the network. The devices that decode the source signal become part of first OLA. The devices of the first OLA retransmit the source signal at the same time without coordinating with each other. The radio devices that decode the signal sent by the nodes of first OLA declare themselves as the members of the second OLA. This procedure continues until the message receives at the destination, where different combining techniques in order to achieve diversity, such as maximum combining ratio (MRC), equal gain combining ratio (ERC), etc., can be applied to get spatial diversity. Because of this diversity gain at the destination, the message signal can reach far distances without draining the entire source power.

1.1.2 OLAPRISE

OLA with Primary Route Setup (OLAPRISE) uses conventional non-cooperative transmission, i.e., single input single output (SISO) transmission for the new path setup/discovery, but for transmitting the source data, it performs OLA transmissions [22]. The cooperative transmission of OLA can be achieved by using one hop neighbors of the devices involved in primary SISO path setup. The setup of this new path can be achieved in a similar fashion to ad hoc on demand distance vector (AODV) routing scheme, which includes route request (downlink) and route reply (uplink), followed by data transmissions and acknowledgements.

1.1.3 OLAROAD

OLA Routing On-demand (OLAROAD) achieves cooperative transmissions using a three step mechanism [23]. In the first step, it broadcasts the route request towards the destination. This broadcast is similar to the basic OLA. The destination when receives the route request (RREQ), unicast the route reply (RREP) message in the backward direction towards the source. The intermediate nodes that receive and decode the RREP, take part in data transmissions from the source to the destination in the third step.

Although OLAROAD gives slightly better performance in terms of latency and throughput, the efficiency of OLAPRISE is found to be better than OLAROAD in the context of low devices involved in OLAPRISE, thus resulting in more energy optimized routes, especially in a situation when a

lot of devices are present in the network. This makes OLAPRISE a desirable form of strip-shaped networks with cooperative transmission.

1.2 Need for Duty Cycling in OLA Networks

In a sensor network, multiple source-destination pairs can exist. A problem may arise when all the pairs want to communicate with each other at the same time. It may happen that the intermediate nodes that contribute in one source-destination path also contribute in another path. Therefore, for all the paths to work properly, each path must have a unique schedule, and all the transmissions take place according to the schedules assigned. These schedules must be time multiplexed in such a way that when one path is transmitting, the other paths go in a silent mode.

1.3 Introducing Additional Stages in OLAPRISE

In order to perform duty cycling in large scale multi-hop OLA networks, we introduce two new stages in the primary OLAPRISE protocol in order to ensure interference free transmissions in the network. The details of each stage is discussed below.

1.3.1 Polling Query

In the primary OLAPRISE, an additional stage in the route setup can be introduced to accommodate a polling task for determining the schedules of the radio nodes across the network. This stage involves the polling of all the

radio nodes inside and around the strip-shaped route to determine whether any of them is part of another stripped route or not.

The ideal time to do polling is when all the nodes that are part of the strip network in OLAPRISE are awake. Therefore, the polling query should be performed right after the Route Reply step of the route discovery process.

1.3.2 Schedule Assignment

The destination node when receives this query packet, detects the schedules that are already occupied in the network. In reply to this polling query, the destination node assigns a new schedule (that is not in use) to its corresponding source by propagating a message in the backward direction towards the source on the already established route. Through this message, the intermediate nodes also know their schedule for this new path.

1.4 Thesis Motivation

Our motivation in this thesis is basically to achieve interference free network, therefore, the reason for finding the schedules flowing in a multi-hop OLA network is to tell the newly established source-destination pair to avoid transmitting in the pre-existing schedules. Whenever, a new source-destination pair desires to communicate with each other, it first finds the schedules running in the network, and then starts its transmission in a new schedule which any other path is not using.

1.5 Thesis Contribution

This thesis presents the following main contributions:

- We study the problem of binary polling of sensors using a cooperative approach where all sensors transmit their decision to the central base station (BS) in one-shot, i.e., at the same time, using diversity channels as in orthogonal frequency division multiple access (OFDMA).
- In the proposed approach, the statistics of the squared envelopes of the received signals, in the line-of-sight as well as in the non line-of-sight channels, are studied to perform hypothesis testing using the Neyman-Pearson criteria.
- We also propose a physical layer approach for detecting the multiple schedules flowing in a cooperative multi-hop linear network.
- For duty cycling and multiple flows scheduling in a dense M2M network, we solve the problem by using irreducible Markov chain in discrete time.

1.6 Thesis Organization

The organization of the thesis is presented as follows. Chapter 2 highlights the literature review of the important concepts proposed in this thesis for providing a flow for the readers. In chapter 3, a well-known detection problem, known as binary integration problem, is investigated, where a set of nodes transmit an event detection message to a destination using orthogonal frequency division multiple access (OFDMA) scheme. This problem has

been solved using the tools from detection theory such as Neyman Pearson Criterion and by studying the receiver operating characteristics (ROC). Chapter 4 presents the problem of detecting multiple Schedules in a cooperative multi-hop linear network using Markov chains. An OFDM packet with orthogonal sub-carriers is considered here to record the information of multiple flows present in the network. The problem is studied using three different approaches in order to perform duty cycling. Chapter 5 discusses the results found in chapter 3 and 4. Finally, chapter 6 presents the conclusions and proposes the future work in this domain.

Chapter 2

Literature Review

Wireless and ad hoc sensor networks have gained popularity in the past decade owing to a multitude of benefits they offer such as low cost, easy deployment, and energy-efficient operations [24–28]. A basic purpose of deploying a sensor network is to gather information from a specific environment and to use this information to build a smart system. The basic idea behind this information exchange is the use of cooperative communication in wireless sensor networks. In literature different strategies for cooperative transmission have been proposed [29–33]

Cooperative communication is a physical layer approach that provides cooperative gains to the destination with an advantage of signal-to-noise (SNR) ratio of 10 to 20 dB [34–36]. Due to these advantages, the system reliability increases with an extra amount of decrease in transmit powers of the source node as compared to the single node scenario.

In [37], the one dimensional network is considered with two different types of node deployments. For the first case, the nodes are placed equidistant from

each other while in the second case, the nodes are co-located with each other. The analytical model here shows the better performance for the co-located scenario. The authors in [38] have studied a strip-shaped linear network with the help of quasi-stationary Markov chain. In [39], the work done in [38] is extended and the effect of composite shadowing has been introduced in the system model.

A two-dimensional (2D) network is considered in [40], in which the authors have extended the work done in [39] and placed two nodes in a single level. The probability of the message to reach the maximum hop distance is determined for the different values of signal-to-noise (SNR) ratio. In [41], a network with random node deployment i.e., the nodes in this network are placed randomly using a Bernoulli distribution, is considered. The network coverage is analyzed by considering a discrete time Markov chain model, with Rayleigh faded channel. The results are compared with a regular node deployment scenario.

In [42], a cooperative multi-hop strip network is studied by considering a fixed boundary between the nodes level. The nodes in each level are assumed constant but the placement of each node is randomized. The coverage probability is determined at the destination node by considering the Weibull distribution for the distance. The authors in [43] have evaluated the timing synchronization errors by considering a multiple input multiple output (MIMO) system, where cooperation among the nodes is employed by implementing decode and forward (DF) protocol.

A linear strip-shaped network is considered in [44], where the nodes deployment is considered with the help of a Poisson point process (PPP). The

probability distribution function (pdf) of the received energy at a particular node is derived, which helps in finding the outage of the nodes transmissions. The network performance in the context of success probability of one hop is investigated in the presence of Rayleigh fading channels.

In [45], a two dimensional (2D) network is studied in order to investigate the intra-flow interference which happens due to the movement of multiple packets in the network. The system model is studied using discrete time Markov chain and the results are derived considering various network parameters. However, the results reveal that the intra-flow interference greatly depends on the SNR. Therefore, the network performance can be optimized by using the higher values of SNR and with improved array gain.

In [46], the authors have considered the two 2D networks such that the information sent by the each source node is totally independent to each other. The destination in this case is a single node located at a very far distance. The concept of network coding is implemented here for merging the two sources information into one. This information then travels with the help of cooperative communication to a far away destination. The model is studied using a quasi-stationary Markov chain in the NLOS channel. The network performance is analyzed by using a state distribution at each node in terms of outage probability for varying values of SNR.

In sensor networks, energy conservation is the key parameter for increasing the network lifetime. The best way to conserve energy is to introduce duty cycle MAC protocols in the network. These protocols conserve energy by controlling the nodes to go on ON and OFF states. The nodes go active when they have data to send or receive. Otherwise, they are in sleep mode.

In literature, many asynchronous and synchronous duty cycle protocols are presented [47–51] in order to ensure energy conservation and to increase the health of a network. The main disadvantage in using these protocols is the packet delay as they require many cycles to reach the destination. [52–56] propose a promising MAC protocol called sensor MAC (S-MAC). S-MAC helps in avoiding collisions and conserving energy in the network, but the main objective of this protocol is to conserve energy in the network. This protocol helps to reduce energy consumption by controlling the sensor nodes to avoid listening in the idle state, i.e., during the idle time, the node goes in the sleep mode.

The conventional binary polling strategy is to communicate all sensor decisions, one at a time, to the collector or BS, which indicates a detection if at least M out of N sensors have detected the event. For instance, [57] and [58] deal with the variation of this problem in distributed detection scenarios but no channel-based solutions have been studied in these papers. The threshold for detecting an event is found optimally by considering both the individual binary sensors as well as the receiver, however, ignoring the channel conditions. Similarly, in [59] and [60], a slight variation is performed in the binary integration problem to achieve time and energy efficiency. In [59], sensors are ranked according to their detecting values depending on the local thresholds for the individual sensors and a subset of sensors are allowed to transmit to the collector. In [60], only the sensor that has the highest detection value transmits its decision to the receiver.

The previous works in the literature do not consider the wireless medium between the sensor nodes and the BS and/or they pay a price in terms of

energy and delay by requiring medium access control (MAC) layer strategies that include channel sensing, listening, and duty cycling of transmissions [61]-[62]. Similar works can be found in [63]- [64], however, the authors either revert to MAC layers, or they don't exploit the feature of diversity in wireless systems.

The authors in [65,66] have presented the method for the detecting different types of informations flowing in the network by using timing analysis, which is quite cumbersome and the purpose of their study is mostly to detect the involvement of intruder with in a system. Moreover, in [67], a channel aware scheduling in the orthogonal frequency division multiplexing (OFDMA) mobile systems is performed to design an intelligent medium access control (MAC) in the downlink channel.

Chapter 3

One Shot Polling of Wireless Sensors

This chapter considers the polling of a sensor network using a binary integration scheme. Binary integration is the combination of binary decisions from multiple sensors into a single decision at the base station. The proposed approach accomplishes binary integration in the physical layer in just two packet intervals regardless of the number of sensors, as long as the sensors are within the decoding range of the collector. We assume independent Rayleigh or Ricean links from the sensor devices to the collector. In the proposed method, the devices simultaneously transmit their signals in each channel of a set of orthogonal channels to create diversity. The statistics of the squared envelopes of the received signals, in both LOS and NLOS channels, are used to perform hypothesis testing using the Neyman-Pearson criteria. It has been shown through the receiver operating characteristic (ROC) curves that the detection probability strongly relies on the number

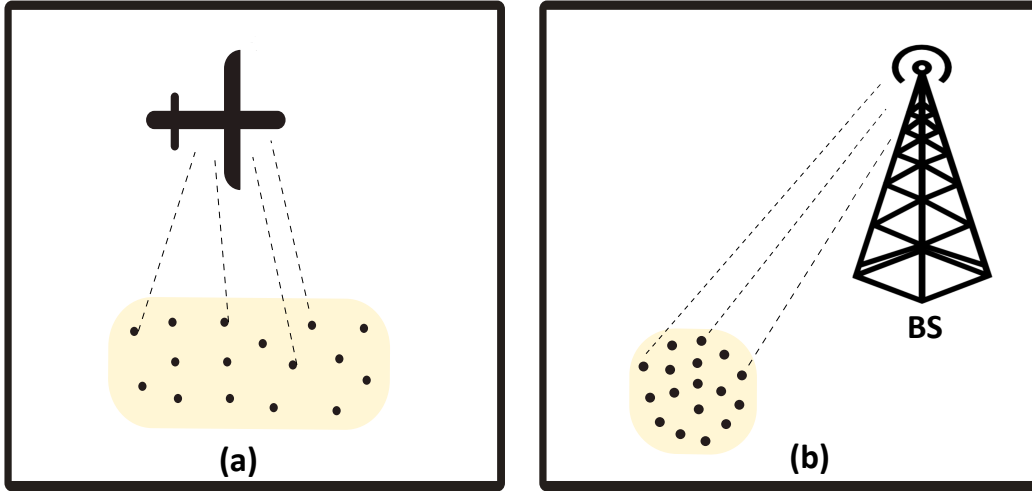


Figure 3.1: (a) An airborne collector receiving the information from the sensors on ground (b). BS receiving the information from a co-located cluster of sensors

of diversity channels available for transmission.

3.1 System Model

The system model is presented here for binary polling where we assume N sensors report their decisions on whether an event happened. We assume the sensors are deployed in an area as shown in Fig 3.1. In Fig 3.1(a), an airborne collector receives the information from the sensors on the ground. Similarly, in Fig 3.1(b), the BS receives the information of a co-located cluster of sensors on the ground. In the BS scenario, the channel model consists of either the NLOS or LOS propagation medium. The number of sensors that decide in the favor of the occurrence of event is S_1 and the number of sensors that decide that an event has not occurred is S_2 .

Under the proposed polling scheme, we assume our polling packet to be

consistent with an OFDM symbol that contains K orthogonal sub-carriers. A sensor that has detected an event transmits in each of the K_1 orthogonal channels that compose the detection band, \mathbb{D} , whereas a sensor that has not detected the event transmits in each of a separate set of K_2 orthogonal channels that compose the non-detection band, $\mathbb{N}\mathbb{D}$, such that $K_1 + K_2 = K$. The sensors' transmissions can be scheduled based on a trigger packet sent by the collector or BS [68] or scheduled for simultaneous transmission, if the network is synchronous. Let $|R_k|^2$ be the squared envelope of the received signal in orthogonal channel k , expressed as

$$|R_k|^2 = |G_k + W_k|^2, \quad (3.1)$$

where G_k is the sum of the complex gains of the sensors' signals in the k^{th} channel and W_k is the noise term for channel k . The elements of W_k are independent and identically distributed (i.i.d) complex Gaussian random variables (RVs) with zero mean and variance σ_n^2 . Let $|R_D|^2$ be the squared envelopes sum of the K_1 receiver branches in the detection band, and similarly $|R_{ND}|^2$ be the sum of the squared envelopes of the K_2 branches in the non-detection band, expressed as

$$|R_D|^2 = \sum_{k \in \mathbb{D}} |R_k|^2 \quad \text{and} \quad |R_{ND}|^2 = \sum_{k \in \mathbb{N}\mathbb{D}} |R_k|^2. \quad (3.2)$$

After receiving the signals from the sensors, the collector makes a detection decision by comparing a threshold with the ratio of the likelihoods of $|R_D|^2$ and $|R_{ND}|^2$. We denote the probability of detection as P_D and the probability

of false alarm as P_{FA} .

3.2 Statistics of the Received Signals

This section derives the statistics of the received message signals for both LOS and NLOS channels as given below.

3.2.1 Non Line-Of-Sight (NLOS) Channel

In the NLOS case, when S_1 sensors are transmitting in each sub-carrier, the G_k in (3.1) is considered as a zero mean complex Gaussian RV, implying its squared envelope, $|G_k|^2$, is given as exponential with mean γS_1 , i.e., $G_k \sim \mathcal{CN}(0, \gamma S_1)$, $|G_k|^2 \sim \exp(\gamma S_1)$, where γ denotes the signal power of each sensor. Similarly from (3.1), the squared envelope $|R_k|^2$ becomes an exponential RV, i.e., $|R_k|^2 \sim \exp(\gamma S_1 + \sigma_n^2)$, thereby implying a signal-to-noise ratio (SNR) of $\gamma S_1 / \sigma_n^2$ for the k th channel. From (3.2), the squared envelopes $|R_D|^2$ and $|R_{ND}|^2$ are, therefore, gamma distributed each having shape parameters K_1 and K_2 with scale parameters $\sigma_1^2 = \gamma S_1 + \sigma_n^2$ and $\sigma_2^2 = \gamma S_2 + \sigma_n^2$, respectively.

We assume that G_k and G_j for $j \neq k$, are i.i.d. The supposition is justified if the K_i sub-carriers have a minimum separation of at least the coherence bandwidth or, in a flat fading channel, if each sensor puts a random phase rotation on *each* of the sub-carriers it excites and there are a sufficient number of excited sub-carriers to assume a central limit theorem approximation.

3.2.2 Line-Of-Sight (LOS) Channel

In the LOS case, we assume that all the S_1 signals in one sub-carrier are i.i.d complex Gaussian with the same non zero mean. Note that the i.i.d assumption is justified if the excited sub-carriers are separated by at least the coherence bandwidth and if each sensor adjusts its carrier phase to ensure the phase of the LOS component at the receiver is the same for all sensors.

Hence, G_k becomes a complex Gaussian RV, i.e.,

$G_k \sim \mathcal{CN}(\mu S_1, \gamma S_1)$, where μ denotes the mean of a signal per sensor. It follows that $|G_k|$ is a Ricean RV with κ factor, $\kappa = S_1 \mu^2 / \gamma$. Since $W_k \sim \mathcal{CN}(0, \sigma_n^2)$, the $|R_k|^2$ becomes a non-central Chi-squared RV, with the following parameters,

$$\alpha = 2S_1\gamma - 3\Delta^2 + \Lambda + 2\sigma_n^2 + S_1^2\mu^2 - \Phi, \quad (3.3)$$

and

$$\beta = 3\Delta^2 - S_1\gamma - \Lambda - \sigma_n^2 - \frac{1}{2}S_1^2\mu^2 + \Phi, \quad (3.4)$$

where $\Delta = \frac{1}{2}(S_1\gamma + \sigma_n^2)$, $\Lambda = \frac{1}{4}(\frac{1}{2}S_1^2\mu^2 + S_1\gamma + \sigma_n^2)^2$ and $\Phi = \frac{1}{16}S_1^4\mu^4 + \frac{3}{2}S_1^2\mu^2\Delta$. It can be shown that the mean and the variance of this non-central Chi-squared RV can be given as $\alpha + \beta$ and $2(\alpha + 2\beta)$, respectively. The mean can be represented in a simplified form as $\frac{1}{2}S_1^2\mu^2 + S_1\gamma + \sigma_n^2$. From (3.2), the squared envelopes $|R_D|^2$ and $|R_{ND}|^2$ are each sums of non-central Chi-squared random variables. It is well known that non-central Chi-squared distribution involves a non-linear Bessel function. Therefore, the distribution of the sum of non-central Chi-squared RVs becomes prohibitive analytically [69]. In the

sequel, we approximate this sum distribution to a gamma distribution using the method of moments approach and also verify the approximation using Kolmogorov-Smirnov (K-S) test [70].

Lemma 1: Let $U = X_1 + X_2 + \dots + X_n$ be the sum of n i.i.d non-central Chi-squared RVs where each RV $X_i, \forall i \in \{1, 2, \dots, n\}$ has identical parameters α and β , then U can be approximated by a gamma RV with shape parameter $\lambda = \frac{n(\alpha+\beta)^2}{2(\alpha+2\beta)}$ and scale parameter $\theta = \frac{2(\alpha+2\beta)}{\alpha+\beta}$, with distribution,

$$f_U(u) = \frac{u^{\lambda-1} \exp\left(\frac{-u}{\theta}\right)}{\theta^\lambda \Gamma(\lambda)}, \quad (3.5)$$

Proof: The mean and variance of the sum of i.i.d. non-central Chi-squared RVs can easily be found as $n(\alpha + \beta)$ and $2n(\alpha + 2\beta)$, respectively [71]. For the moment matching approach, we equate two moments of both the distributions as

$$\mathbb{E}[|R_k|^2] = n(\alpha + \beta) = \lambda\theta = \mathbb{E}[U], \quad (3.6)$$

$$\text{Var}[|R_k|^2] = 2n(\alpha + 2\beta) = \lambda\theta^2 = \text{Var}[U]. \quad (3.7)$$

Solving the above equations provide us the shape parameter λ and scale parameter θ for RV U as

$$\lambda = \frac{n(\alpha + \beta)^2}{2(\alpha + 2\beta)} \quad \text{and} \quad \theta = \frac{2(\alpha + 2\beta)}{\alpha + \beta}. \quad (3.8)$$

The second step involves performing the K-S test for the goodness of fit of

the distributions. The K-S test can be used to compare the sample distribution with some reference distribution [72]. The test is performed by taking the samples $(\zeta_1, \zeta_2, \dots, \zeta_\Omega)$ from both the distributions and the maximum distance between the cumulative distribution function (CDF) $F_1(\zeta)$ of reference distribution and empirical distribution function $F_0(\zeta)$ of sample distribution is found using these samples. The test is performed by making two hypotheses: \mathcal{H}_0 (null hypothesis) and \mathcal{H}_1 (reject hypothesis). The null hypothesis says that the samples of both the distributions are from the same distribution, i.e.,

$$\mathcal{H}_0 : F_1 = F_0, \quad (3.9)$$

whereas the hypothesis \mathcal{H}_1 rejects the null hypothesis. The maximum difference between the CDFs is given as

$$\hat{D}_f = \max_i |F_1(\zeta_i) - F_0(\zeta_i)|. \quad (3.10)$$

The K-S test also depends on the significance level, ε , of the test, which is defined as the probability of rejecting \mathcal{H}_0 given that the two distributions are the same, i.e.,

$$\varepsilon = \mathbb{P}(\hat{D}_f \geq c | \mathcal{H}_0), \quad (3.11)$$

where c defines the critical value and it depends on number of samples Ω as well as ε . The null hypothesis is accepted only if $\hat{D}_f \leq c$.

The K-S tests performed for different number of samples, Ω , and for sums of 100 and 1000 non-central Chi-squared RVs with $\varepsilon = 0.05$, $S_1 = 100$, $\gamma = 2$, $\mu = 4$ and $\sigma_n^2 = 1$ are given in Table 3.1. The values of c can be found from

Table 3.1: K-S test for CDF approximations.

No: of Samples (Ω)	Value of c	$\hat{D}_f, n = 100$	$\hat{D}_f, n = 1000$
3000	0.024	0.0146	0.0218
4000	0.021	0.0180	0.0103
5000	0.019	0.0172	0.0083
6000	0.017	0.0111	0.0104

the table given in [72]. The findings in Table 3.1 show that the value of \hat{D}_f is always less than the value of c , which implies that the sum of non-central Chi-squared RVs can be well approximated as a gamma RV.

Hence the distributions of $|R_D|^2$ and $|R_{ND}|^2$ are approximated as gamma distribution, with shape and scale parameters $\lambda_i = \frac{K_i(\alpha_i + \beta_i)^2}{2(\alpha_i + 2\beta_i)}$, and $\theta_i = \frac{2(\alpha_i + 2\beta_i)}{\alpha_i + \beta_i}$ for $i = \{1, 2\}$, respectively.

3.3 Neyman-Pearson Detection Tests

This section performs the NP tests for both LOS as well as NLOS channels as given below.

3.3.1 NP Test for the NLOS Channel

For detection, the Neyman-Pearson method is employed, which states that the alternative hypothesis is decided if

$$\frac{p(x; \mathcal{H}_1)}{p(x; \mathcal{H}_0)} > \tau. \quad (3.12)$$

In (3.12), \mathcal{H}_0 is the null hypothesis and \mathcal{H}_1 is the alternative hypothesis and τ is the threshold. From the previous section, $p(x; \mathcal{H}_0) \sim \text{Gamma}(K_2, \sigma_2^2)$

and $p(x; \mathcal{H}_1) \sim \text{Gamma}(K_1, \sigma_1^2)$. Hence, (3.12) can be written as

$$\frac{\frac{x^{K_1-1} \exp\left(\frac{-x}{\sigma_1^2}\right)}{\sigma_1^{2K_1} \Gamma(K_1)}}{\frac{x^{K_2-1} \exp\left(\frac{-x}{\sigma_2^2}\right)}{\sigma_2^{2K_2} \Gamma(K_2)}} > \tau. \quad (3.13)$$

Further simplification provides

$$\frac{x^{K_1-1} \exp\left(\frac{-x}{\sigma_1^2}\right) \sigma_2^{2K_2} \Gamma(K_2)}{x^{K_2-1} \exp\left(\frac{-x}{\sigma_2^2}\right) \sigma_1^{2K_1} \Gamma(K_1)} > \tau. \quad (3.14)$$

Solving and rearranging (3.14), we get

$$\begin{aligned} (K_1 - K_2) \ln(x) + \left(\frac{\sigma_1^2 - \sigma_2^2}{\sigma_1^2 \sigma_2^2} \right) x &> \ln(\tau) + K_1 \ln(\sigma_1^2) \\ &+ \ln \Gamma(K_1) - K_2 \ln(\sigma_2^2) - \ln \Gamma(K_2). \end{aligned} \quad (3.15)$$

General Case

Solving for x , we get the general solution as

$$x > \frac{A \mathcal{W}\left(\frac{B e A^C}{B}\right)}{B} := t_1, \quad (3.16)$$

where $\mathcal{W}(\cdot)$ is Lambert-W function, $A = (K_1 - K_2)$, $B = \left(\frac{\sigma_1^2 - \sigma_2^2}{\sigma_1^2 \sigma_2^2} \right)$ and $C = \ln(\tau) + K_1 \ln(\sigma_1^2) + \ln \Gamma(K_1) - K_2 \ln(\sigma_2^2) - \ln \Gamma(K_2)$. The above equation is true only for $\sigma_1^2 > \sigma_2^2$.

Case 1a

In (3.15), when $K_1 = K_2$, (3.19) simplifies to

$$x > \frac{\ln(\tau) + K \ln(\sigma_1^2) - K \ln(\sigma_2^2)}{\left(\frac{\sigma_1^2 - \sigma_2^2}{\sigma_1^2 \sigma_2^2}\right)} := t_2. \quad (3.17)$$

Case 1b

Similarly in (3.15), when $\sigma_1^2 = \sigma_2^2$, we will have a different solution for x as

$$x > \exp\left(\frac{\ln(\tau) - (K_2 - K_1)\ln(\sigma_1^2) + \psi}{K_1 - K_2}\right) := t_3, \quad (3.18)$$

where $\psi = \ln\Gamma(K_1) - \ln\Gamma(K_2)$. The probability of false alarm P_{FA} and the probability of detection P_D for each case can now be determined as

$$P_{FA} = \int_{t_i}^{\infty} p(x; \mathcal{H}_0) dx, \quad i \in \{1, 2, 3\} \quad (3.19)$$

and

$$P_D = \int_{t_i}^{\infty} p(x; \mathcal{H}_1) dx \quad i \in \{1, 2, 3\}. \quad (3.20)$$

3.3.2 NP Test for the LOS Channel

In the LOS case, the distributions of $|R_D|^2$ and $|R_{ND}|^2$ are approximated as gamma distributions; therefore, the Neyman-Pearson test is conducted in the same manner as in the NLOS case and follows the same steps as done in (3.12) to (3.15), where we can replace the σ_1^2 and σ_2^2 with λ_1 and λ_2 and K_1 and K_2 with θ_1 and θ_2 , respectively.

Chapter 4

Polling of Sensors in a

Multi-hop M2M Network

The work done in the previous chapter 3, is extended here to a multi-hop scenario in which a linear strip-shaped network is considered. The schedules present in the network are determined using an OFDM packet transmission from source node to the far away destination using three different techniques. The analytical results are derived by modeling the sensors transmission with a discrete time Markov chain.

4.1 System Description

Consider a large-scale M2M network, where multiple source-destination pairs exist and multi-hop routes have been formed between each source-destination pair. The nodes in each route are arranged in a line forming a one-dimensional linear network as shown in Fig. 4.1. This implies that for each route, a sin-

gle node is present in each hop, constituting a SISO multi-hop scenario. We now assume that a new pair of source-destination appears in the network, as shown in Fig. 4.1 in the horizontal route, which happens to cross one or more already established paths. For instance, in Fig. 4.1, the new route crosses two established routes represented by two vertical paths. The destination node is located m hops away from the source node as shown in Fig. 4.1. We assume that in this new source-destination path, a node is present after every n_i hops that is already part of an existing route, and hence follows a certain schedule $s \in \mathcal{S}$ from the set $\mathcal{S} = \{1, 2, \dots, S\}$, where S defines the total number of schedules present in the network at one time.

Recall that our objective in this thesis is to assign an orthogonal schedule to this new route so that the nodes sleep and wake in such a manner that there is no interference on them. For the example given in Fig. 4.1, the new route should follow any schedule other than $\{1, 2\}$ because they are currently in use. The source in this case initiates a polling query, which travels all the way to the new destination. The purpose of this polling query is to get the information of all schedules that the nodes of this route follow. The intermediate nodes, present in this new path, when receive this polling query, insert the information of the schedules that they follow. The destination node when receives this query packet, detects the schedules that are already occupied in the network. In reply to this polling query, the destination node assigns a new schedule (that is not in use) to its corresponding source by propagating a message in the backward direction towards the source on the already established route. Through this message, the intermediate nodes also know their schedule for this new path.

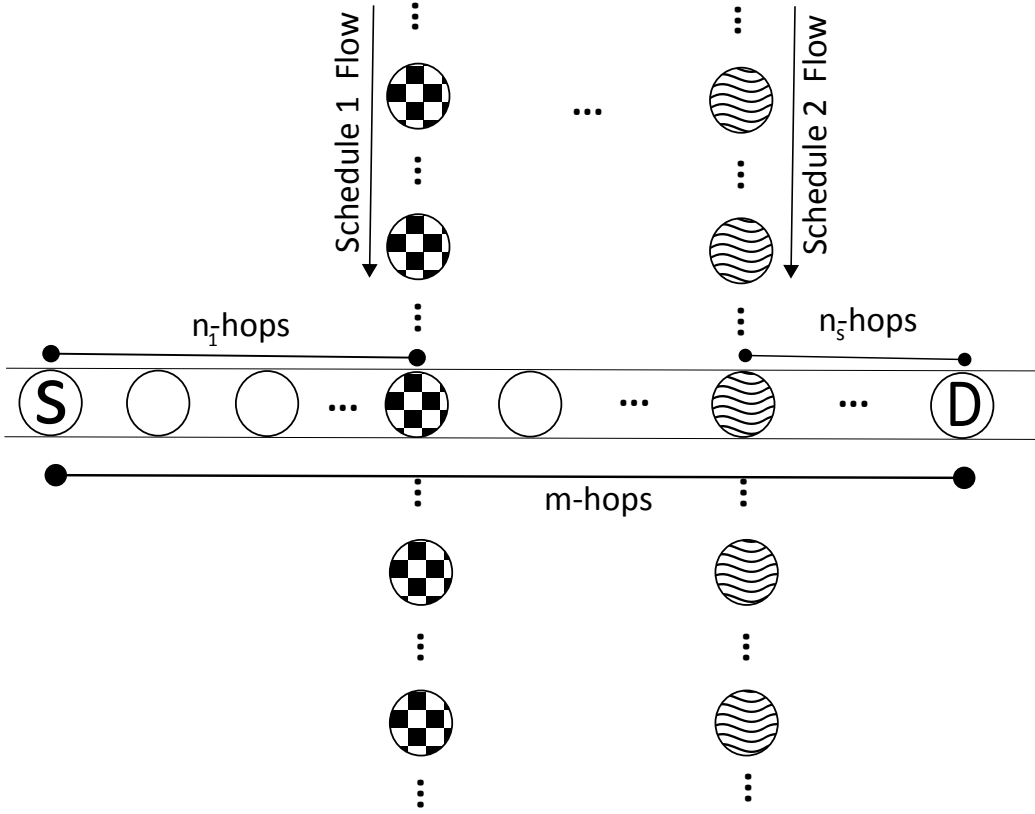


Figure 4.1: The system model showing a new source-destination route crossing two already existing routes.

For the detection of existing schedules at the new destination node, we consider our source packet to be consistent with an OFDM symbol. The total number of orthogonal sub-carriers in an OFDM packet are KS , where $K \in \mathbf{Z}^+$, i.e., a positive integer. These sub-carriers are divided into S bands in such a way that for every schedule i , there is a band B_i . Each band contains K number of sub-carriers, which are used to report the information of one particular schedule. For the example shown in Fig. 4.1, we suppose that the total number of schedules present in the network are 4, i.e., $S = 4$. The OFDM packet in this case contains 4 bands as shown in Fig. 4.2. Let

the number of sub-carriers K , assigned to each band are 3. The overall packet, therefore, consists of 12 sub-carriers. Here, the band B_1 is reserved for schedule 1, B_2 for schedule 2, and so on. The source initiates the polling process by transmitting a binary phase shift keying (BPSK) symbol 0 in all the bands, implying that the source is not part of any existing schedule. When the first node receives this packet, it employs energy detection to detect the presence/absence of symbols in each sub-carrier of the received OFDM packet. If the symbols present in a band, representing a certain schedule, are decoded correctly, then that schedule is detected successfully. Otherwise, incorrect decoding of the symbols representing a certain schedule causes false alarms in the network. Because of this false alarm, a schedule that is absent in the network, appears to be detected. When a node that follows a schedule s receives this OFDM packet, it performs energy detection in each sub-carrier and inserts a BPSK symbol 1 in all the sub-carriers corresponding to the B_s band. On the other hand, in rest of the bands, the node propagates the previous information obtained after performing energy detection. For the case discussed in Fig. 4.1 and Fig. 4.2, when the node that follow schedule 1 receives an OFDM packet, it inserts its schedule information by transmitting BPSK symbol 1 in all the sub-carriers of B_1 band and in the rest of the bands, the previous information propagates, as obtained through energy detection. Similarly, when the node following schedule 2 receives this packet, it transmits BPSK symbol 1 in all the sub-carriers of B_2 band, and propagates the previous information in rest of the bands. The destination node when receives this packet, detects that the schedule 1 and 2 are already occupied in the network. Hence, it assigns an orthogonal schedule such as

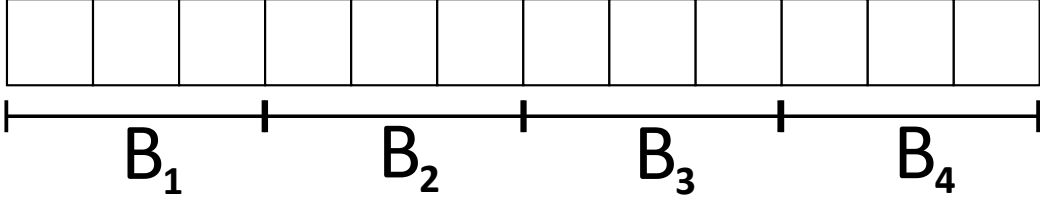


Figure 4.2: The OFDM packet with 12 sub-carriers, i.e., $S = 4$ and $K = 3$.

3 or 4 to the source node. If because of the false alarms, schedule 3 is also detected at the destination, then the destination node asks the source node to follow schedule 4.

Here we assume that the total power required for an OFDM packet transmission is P . The transmit power per sub-carrier is then defined as P_t i.e., $P_t = \frac{P}{K \times S}$. Here we also assume that all the channels are Rayleigh fading. The message travels all the way to the destination through multiple hops. For a node in a level l , the signal received at any sub-carrier j of the OFDM packet is given as

$$y_j = \sqrt{P_t} h_j x_j + n_j, \quad (4.1)$$

where h_j is the channel gain, which is a zero mean and unit variance complex Gaussian RV, i.e., $h_j \sim \mathcal{CN}(0, 1)$ corresponding to Rayleigh fading, $n_j \sim \mathcal{CN}(0, N)$ is the noise in j th sub-carrier with variance N and x_j is the BPSK symbol 0 or 1. The energy in a sub-carrier j is thus exponentially distributed, i.e., $|y_j|^2 \sim \exp(\lambda)$, where $\lambda = P_t + N$, with the probability distribution function (PDF) given as

$$f_{|y_j|^2}(y) = \frac{1}{\lambda} \exp\left(\frac{-y}{\lambda}\right). \quad (4.2)$$

4.2 Modeling by Markov Chain

At any level l , since the total number of schedules present in a network are S , so the total possible packet states are 2^S . The OFDM packet received by a radio node belongs to any of the possible states depending upon the schedules detected. The packet states are defined as

$$\mathbb{Y}(l) = [\mathbb{X}_1(l), \mathbb{X}_2(l), \dots, \mathbb{X}_S(l)], \quad (4.3)$$

where $\mathbb{X}_i(l)$ is the binary indicator random variable for i th schedule at level l , given as

$$\mathbb{X}_i(l) = \begin{cases} 1 & \text{if } i\text{th schedule is detected} \\ 0 & \text{if } i\text{th schedule is not detected} \end{cases} \quad (4.4)$$

The detection of each schedule, i.e., the value of $\mathbb{X}_i(l)$ itself dependent on the detection of the received signal energy in each of the K sub-carriers, assigned to that schedule. We follow three different cases as described here to get the value of $\mathbb{X}_i(l)$.

4.2.1 Strict Approach

In this approach, a schedule s is detected only when the received signal energy in each of the individual K sub-carriers of the B_s band is greater than some energy threshold τ . If the received energy in any of the K sub-carriers is less than τ , then the schedule is assumed to be not detected. The probability of

detection of one sub-carrier, j , is given as

$$\mathbb{P}_d = \mathbb{P}\{|y_j|^2 > \tau\}, \forall j \in \{1, 2, \dots, K\}, \quad K \in B_s. \quad (4.5)$$

Thus, for the strict case, the probability of detection of one schedule, s , is defined as

$$\mathbb{P}_s^{(s)} = \prod_{j=1}^K \mathbb{P}\{|y_j|^2 > \tau\}, \quad K \in B_s, \quad (4.6)$$

$$\mathbb{P}_o^{(s)} = 1 - \prod_{j=1}^K \mathbb{P}\{|y_j|^2 > \tau\}, \quad K \in B_s, \quad (4.7)$$

where $\mathbb{P}_s^{(s)}$ and $\mathbb{P}_o^{(s)}$ denote the probability of successful detection and probability of outage, respectively, of the schedule s .

4.2.2 Lenient Approach

In this case, a schedule s is detected when the received signal energy in any of the individual K sub-carriers of the B_s band is greater than some energy threshold τ . The schedule is not detected only in that case, when the received signal energy in all of the K sub-carriers is less than τ . The probability of successful detection, $\mathbb{P}_s^{(s)}$, and probability of outage, $\mathbb{P}_o^{(s)}$, of the schedule s is given as

$$\mathbb{P}_s^{(s)} = 1 - \left(\prod_{j=1}^K \left(1 - \mathbb{P}\{|y_j|^2 > \tau\} \right) \right), \quad K \in B_s, \quad (4.8)$$

$$\mathbb{P}_o^{(s)} = \prod_{j=1}^K \left(1 - \mathbb{P}\{|y_j|^2 > \tau\} \right), \quad K \in B_s. \quad (4.9)$$

4.2.3 Diversity Approach

In this scenario, a schedule s is detected when the combined received signal energy of all the K sub-carriers of the B_s band is greater than some energy threshold τ . The probability of successful detection, $\mathbb{P}_s^{(s)}$ and probability of outage, $\mathbb{P}_o^{(s)}$ of the schedule s is given as

$$\mathbb{P}_s^{(s)} = \mathbb{P}\left\{\sum_{j=1}^K |y_j|^2 > \tau\right\}, \quad K \in B_s, \quad (4.10)$$

$$\mathbb{P}_o^{(s)} = 1 - \mathbb{P}\left\{\sum_{j=1}^K |y_j|^2 > \tau\right\}, \quad K \in B_s. \quad (4.11)$$

From (4.3), we can see that the outcomes of $\mathbb{Y}(l)$ are S -bit binary words, each constituting a state. These states in decimal form are written as $\{0, 1, \dots, 2^S - 1\}$. Let b_l be the outcome of $\mathbb{Y}(l)$ at level l . For example, $b_l = 1010$ in binary indicates 10 in decimal, which implies that the node has detected schedules 1 and 3 in this case. Therefore, $\mathbb{Y}(l)$ can be modeled as a discrete time finite state Markov Process with \mathbb{P} as a probability measure, given as

$$\begin{aligned} \mathbb{P}\{\mathbb{Y}(l) = b_l | \mathbb{Y}(l-1) = b_{l-1}, \dots, \mathbb{Y}(1) = b_1\} = \\ \mathbb{P}\{\mathbb{Y}(l) = b_l | \mathbb{Y}(l-1) = b_{l-1}\}. \end{aligned} \quad (4.12)$$

The packets can go from one transient state to any other transient state, therefore all of the packet states make an irreducible state space as shown in Fig. 4.3. The Markov chain is defined by a probability transition matrix \mathbf{P} of order $(2^S \times 2^S)$, which is defined on the corresponding states in \mathbb{Y} . Each

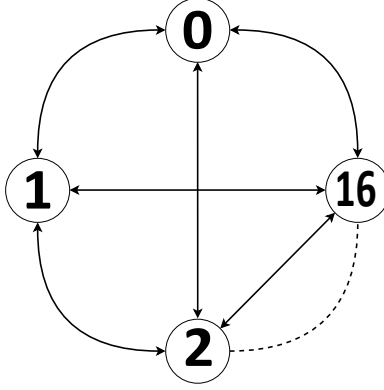


Figure 4.3: The state space representation of $\mathbb{Y}(l)$ for $S = 4$.

row of \mathbf{P} , when summed, gives 1. From the study of Markov chains [73], a distribution $\boldsymbol{\pi} = (\pi_i, i \in \{1, 2, \dots, 2^S\})$ is called v -invariant distribution if $\boldsymbol{\pi}$ is the left eigenvector of the transition matrix \mathbf{P} corresponding to the eigenvalue v , i.e.,

$$\boldsymbol{\pi}\mathbf{P} = v\boldsymbol{\pi}. \quad (4.13)$$

The distribution $\boldsymbol{\pi}$ is a row vector of size (1×2^S) , with the entry π_i corresponding to the probability of occurrence of the state i . Our interest here is to find the distribution $\boldsymbol{\pi}$ of the transient states at each hop. Considering our system model, the distribution $\boldsymbol{\pi}$ at the n th hop can be determined as

$$\boldsymbol{\pi}^{(n)} = \boldsymbol{\pi}^{(0)}\mathbf{P}^{(n)}, \quad (4.14)$$

where $\boldsymbol{\pi}^{(0)}$ is the initial distribution of the source packet. Since, the source node does not follow any schedule, therefore, initially the source packet would be in state 0. This is because the source forwards the OFDM packet with all the sub-carriers filled with BPSK symbol 0. Considering the example discussed in Fig. 4.1 and Fig. 4.2, the state of the packet at the source node is

given as $\mathbb{Y}(0) = [0000]$. Hence, the initial distribution $\boldsymbol{\pi}^{(0)}$ in this case is a row vector of size (1×16) whose first entry is 1 and all other entries are zero represented as $\boldsymbol{\pi}^{(0)} = [1 \ 0 \ 0 \ 0 \ 0 \ 0 \ 0 \ 0 \ 0 \ 0 \ 0 \ 0 \ 0 \ 0 \ 0 \ 0]$. If a node located at the n th hop follows a certain schedule s , then it enters its schedule information, i.e., inserts BPSK symbol 1 in each of the K subcarriers of the B_s band of the previously received OFDM packet. The distribution $\boldsymbol{\pi}^{(n)}$ then modifies to $\hat{\boldsymbol{\pi}}^{(n)}$ according to Algorithm 1. This distribution $\hat{\boldsymbol{\pi}}^{(n)}$ then becomes the initial distribution for finding $\boldsymbol{\pi}^{(n+1)}$. The distribution at the $(n + 1)$ th hop can then be determined as

$$\boldsymbol{\pi}^{(n+1)} = \hat{\boldsymbol{\pi}}^{(n)} \mathbf{P}. \quad (4.15)$$

Thus the packet travels all the way to the destination, which is m hops from the source. We find the distribution $\boldsymbol{\pi}^{(m)}$ at the destination, which gives the information about the occurrence of each schedule in the network.

The working of Algorithm 1 can be explained well by considering an example. Let us assume that a node located at the n th hop follows schedule 2, i.e., $s = 2$, and the total number of schedules present in the network are $S = 4$. The distribution vector $\boldsymbol{\pi}^{(n)}$ obtained at the n th hop is shown at the top in Fig. 4.4. The algorithm defines two sets \mathbf{A} and \mathbf{B} each of size $(1 \times 2^{S-1})$. The value of δ is to be calculated using the formula $\delta = 2^{(S-s)}$, which in this case becomes 4. Depending on the value of δ , the algorithm picks first δ (in this case 4) values from $\boldsymbol{\pi}^{(n)}$ vector and places them into set \mathbf{A} , and the next δ values in set \mathbf{B} . This process continues until the sets \mathbf{A} and \mathbf{B} are filled as shown in Fig. 4.4. These two sets \mathbf{A} and \mathbf{B} are added to

Algorithm 1: Finding Initial Distribution

Input : $\pi^{(n)}$
Output: $\hat{\pi}^{(n)}$

- 1 **initialization**: $i \leftarrow 1, j \leftarrow 1, a \leftarrow 1, b \leftarrow 1$;
- 2 $\mathbf{S} \leftarrow \{1, 2, \dots, S\}$, a set of all schedules;
- 3 $s \in \mathbf{S}$, s is the node schedule;
- 4 \mathbf{O} , zero vector of same size as \mathbf{S} ;
- 5 $\delta := 2^{S-s}$, find value;
- 6 **while** $i \leq 2^S$ **do**
- 7 $\mathbf{A}[a : \delta + a - 1] := \pi^{(n)}[i : \delta + i - 1]$;
- 8 $\mathbf{B}[a : \delta + a - 1] := \pi^{(n)}[\delta + i : 2\delta + i - 1]$;
- 9 $i := 2\delta + i$;
- 10 $a := \delta + a$;
- 11 **end**
- 12 $\mathbf{C} = \mathbf{A} + \mathbf{B}$;
- 13 **while** $j \leq 2^{S-1}$ **do**
- 14 $\hat{\pi}^{(n)}[b : 2\delta + b - 1] := \left[\mathbf{O}[j : j + \delta - 1] \ \mathbf{C}[j : j + \delta - 1] \right]$;
- 15 $j := \delta + j$;
- 16 $b := 2\delta + b$;
- 17 **end**

make a third set \mathbf{C} . A zero vector of the same order as \mathbf{C} is initialized. The modified distribution vector $\hat{\pi}^{(n)}$ is obtained by placing the first δ values from the zero vector and the next δ values from the set \mathbf{C} into $\hat{\pi}^{(n)}$ vector. The same repeats for the other values until the distribution vector completes. The reason for using this Algorithm is due to the fact that when a node receives an OFDM packet, it enters its schedule information in the packet. Because of this, the previous information inside the packet changes, thus, the initial distribution also changes. In order to model a Markov chain, the initial distribution is to be determined at the node for finding the state distribution at the next level.

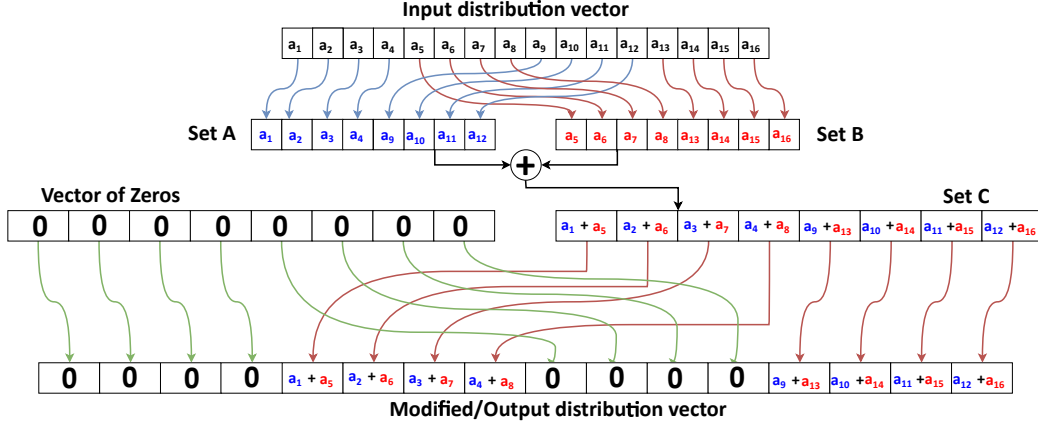


Figure 4.4: The working of Algorithm 1 for $S = 4$, $s = 2$, and $\delta = 4$.

It must be noted, that if a node follows more than one schedule, i.e., $s = 2$ and 3. Then the modified distribution vector can be obtained by following the Algorithm 1 twice. For the first time, we find $\tilde{\pi}^{(n)}$ for $s = 2$, then for the second time, find $\hat{\pi}^{(n)}$ for $s = 3$ using the same $\tilde{\pi}^{(n)}$ obtained in the previous case ($s = 2$), as the input distribution in the Algorithm 1. This $\hat{\pi}^{(n)}$ serves as the initial distribution for finding $\pi^{(n+1)}$ in this case.

4.3 Formulation of the Transition Probability Matrix

The state transition matrix \mathbf{P} is derived in this section for our system model. The state distribution of a packet can easily be obtained by finding the left eigenvector of the \mathbf{P} matrix. Let us assume i and j as a pair representing the states of a packet such that $i, j \in \{0, 1, 2, \dots, 2^S - 1\}$. These states i and j in a S -bit binary word are written as $i = (\beta_{S-1}^{(i)}, \dots, \beta_1^{(i)}, \beta_0^{(i)})$ and $j = (\beta_{S-1}^{(j)}, \dots, \beta_1^{(j)}, \beta_0^{(j)})$, respectively. Since, the probability of detection and

the probability of outage of every schedule in an OFDM packet can be represented using the same mathematical expression, i.e., $\mathbb{P}_s^{(1)} = \mathbb{P}_s^{(2)} = \dots = \mathbb{P}_s^{(s)} = \mathbb{P}_s$ and $\mathbb{P}_o^{(1)} = \mathbb{P}_o^{(2)} = \dots = \mathbb{P}_o^{(s)} = \mathbb{P}_o$, so, the state transition matrix \mathbf{P}_{ij} can be defined as

$$\mathbf{P}_{ij} = \prod_z (\mathbb{P}_o) \cdot \prod_{S-z} (\mathbb{P}_s), \quad (4.16)$$

where $z = \sum_{k=0}^{S-1} (\beta_k^{(i)} \oplus \beta_k^{(j)})$. From (4.5), the probability of detection of one sub-carrier, j , is defined as

$$\mathbb{P}_d = \mathbb{P}\{|y_j|^2 > \tau\} = \int_{\tau}^{\infty} f_{|y_j|^2}(y) dy, \quad (4.17)$$

where τ is the energy threshold. Simplifying the above equation gives

$$\mathbb{P}_d = \exp\left(\frac{-\tau}{\lambda}\right). \quad (4.18)$$

The state transition matrix \mathbf{P}_{ij} , for all the three approaches, is found in the following three cases.

4.3.1 Strict Approach

From (4.6), the probability of successfully detecting a schedule is given as

$$\mathbb{P}_s = (\mathbb{P}_d)^K = \exp\left(\frac{-\tau K}{\lambda}\right), \quad (4.19)$$

where $\lambda = P_t + N$. The probability of outage in this case is found using (4.7) as

$$\mathbb{P}_o = 1 - (\mathbb{P}_d)^K = 1 - \exp\left(\frac{-\tau K}{\lambda}\right). \quad (4.20)$$

The state transition matrix \mathbf{P}_{ij} from (4.16), is written as

$$\mathbf{P}_{ij} = \prod_z \left(\exp\left(\frac{-\tau K}{\lambda}\right) \right) \cdot \prod_{S-z} \left(1 - \exp\left(\frac{-\tau K}{\lambda}\right) \right). \quad (4.21)$$

4.3.2 Lenient Approach

From (4.8), the probability of successfully detecting a schedule is given as

$$\mathbb{P}_s = 1 - (1 - \mathbb{P}_d)^K = 1 - \left(1 - \exp\left(\frac{-\tau}{\lambda}\right) \right)^K. \quad (4.22)$$

The probability of outage using (4.9) is given as

$$\mathbb{P}_o = (1 - \mathbb{P}_d)^K = \left(1 - \exp\left(\frac{-\tau}{\lambda}\right) \right)^K. \quad (4.23)$$

From (4.16), the state transition matrix \mathbf{P}_{ij} is written as

$$\mathbf{P}_{ij} = \prod_z \left(1 - \left(1 - \exp\left(\frac{-\tau}{\lambda}\right) \right)^K \right) \cdot \prod_{S-z} \left(\left(1 - \exp\left(\frac{-\tau}{\lambda}\right) \right)^K \right). \quad (4.24)$$

4.3.3 Diversity Approach

In this approach, the combined energy of all the K sub-carriers is to be determined. The distribution of which is obtained by summing the K exponential RV's with identical mean λ , which is defined as $Gamma(K, \lambda)$ [74]. Here K and λ represent the shape and scale parameters of the Gamma function, respectively. Now, from (4.10), the probability of successfully detecting a

schedule in this case is defined as

$$\mathbb{P}_s = \sum_{p=0}^{K-1} \frac{1}{p!} \left(\frac{\tau}{\lambda}\right)^p \exp\left(\frac{-\tau}{\lambda}\right), \quad (4.25)$$

while the probability of outage of schedule, using (4.11) is given as

$$\mathbb{P}_o = 1 - \left(\sum_{p=0}^{K-1} \frac{1}{p!} \left(\frac{\tau}{\lambda}\right)^p \exp\left(\frac{-\tau}{\lambda}\right) \right), \quad (4.26)$$

The state transition matrix \mathbf{P}_{ij} from (4.16), is therefore written as

$$\mathbf{P}_{ij} = \prod_z \left(\sum_{p=0}^{K-1} \frac{1}{p!} \left(\frac{\tau}{\lambda}\right)^p \exp\left(\frac{-\tau}{\lambda}\right) \right) \cdot \prod_{S-z} \left(1 - \left(\sum_{p=0}^{K-1} \frac{1}{p!} \left(\frac{\tau}{\lambda}\right)^p \exp\left(\frac{-\tau}{\lambda}\right) \right) \right). \quad (4.27)$$

The state transition matrix \mathbf{P}_{ij} thus helps in finding the schedules running in the network.

Chapter 5

Results and Discussions

This chapter presents the results for both the one shot polling of sensor nodes and the polling of sensors in a multi-hop OLA network are analyzed.

5.1 Results for One Shot Polling of Wireless Sensors

This section presents the numerical results obtained through NP tests for both LOS and NLOS channels. Fig. 5.1 provides the ROC curves for P_D versus P_{FA} for equal number of sensors transmitting in the detection and non-detection bands, or $S_1 = S_2$ such that $S_1 + S_2 = 40$, while the number of sub-carriers in the detection band is larger than or equal to the number of sub-carriers in the non-detection band, keeping the total number of diversity channels equal to 30, i.e., $K_1 \geq K_2$ and $K_1 + K_2 = 30$. If $K_1 = K_2$ and $S_1 = S_2$, the detector performance is shown by the linear line at 45° , which is intuitive since there is no majority in the sensors' reports. However, it

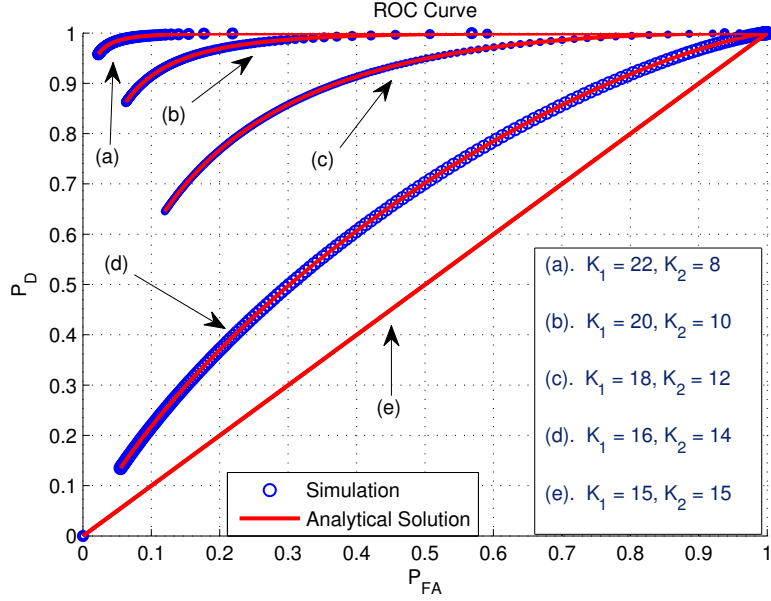


Figure 5.1: The ROC curves for different values of K_1 and K_2 but for same values of S_1 and S_2 , i.e., $S_1 = S_2 = 20$, at 10dB of SNR with NLOS channel

can be seen that if the diversity channels for detection band are increased, then we achieve a higher P_D . In other words, the graph provides an insight into the ‘distortion of truth’ if we increase the diversity channels only in the detection band. A Monte-Carlo Simulation test is also conducted to prove the theoretical model. The figure clearly shows that the theoretical results have a close match with the simulation results, thereby providing the accuracy of our proposed model.

Fig. 5.2 represents the ROC performance for equal number of sub-carriers in both detection as well as non-detection bands, however, varying the number of sensors that report the event happening. The total number of sensors in the area are kept at 100. It can be observed that by increasing the total number of sensors transmissions in the detection band, the P_D increases for

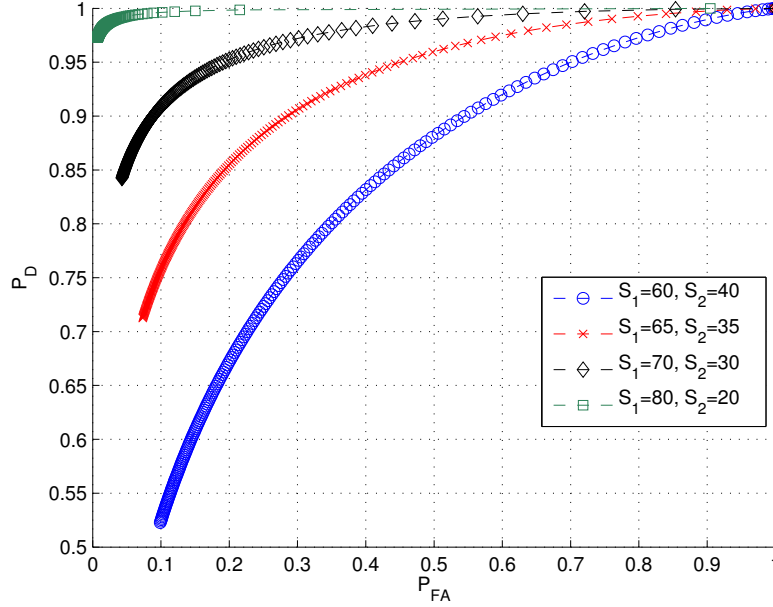


Figure 5.2: The ROC curves for $K_1 = K_2 = 10$ for varying values of S_1 and S_2 at SNR of 10dB in a NLOS channel.

a fixed P_{FA} . This phenomenon can be attributed to the ‘majority voting’ in a binary polling system where the detection probability increases as the number of sensors increases.

Fig. 5.3 shows a contour plot of the probability of detection for a case where $K_1 = K_2 = 10$, and the total number of sensors are 50, i.e., $S_1 + S_2 = 50$, however, their difference is plotted against the SNR. The P_{FA} is kept fixed at 0.05. It can be seen that a high P_D can be achieved by keeping the difference of S_1 and S_2 large, however, operating the system at low SNRs. This is because when many sensors are transmitting in the detection band, the power gain (or array gain) improves the detection probability. Similarly, a high P_D also results when the SNR of the system is high although the margin of the majority, i.e., $S_1 - S_2$, is small. Note that the top right corner

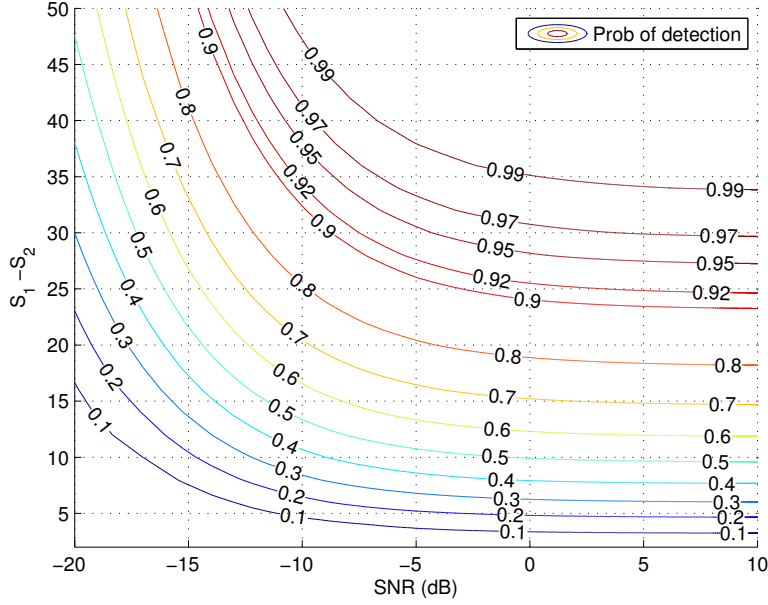


Figure 5.3: Contour plot of probability of detection for varying SNR; $K_1 = K_2 = 10$, and $P_{FA} = 0.05$

of the plot depicts unit P_D .

Fig. 5.4 shows the diversity effects on the performance of detection when the number of sub-carriers across both detection and non-detection bands are the same, however, there are only event reporting sensors in the area. In symbols, this implies $K_1 = K_2$, $S_1 = 5$ and $S_2 = 0$. The plot shows that to get a low detection error, one must resort to increase the number of diversity channels so that the diversity gain starts to play its role. We observe the increasing slopes' characteristic of increasing diversity. For example, the limiting slope of $K_1 = K_2 = 10$ is twice that of $K_1 = K_2 = 5$.

Finally, we also provide results of ROCs for both LOS and NLOS channels at an SNR of 0dB. The Fig. 5.5 here shows that as we increase the κ -factor for the LOS channels, the detection performance also increases .

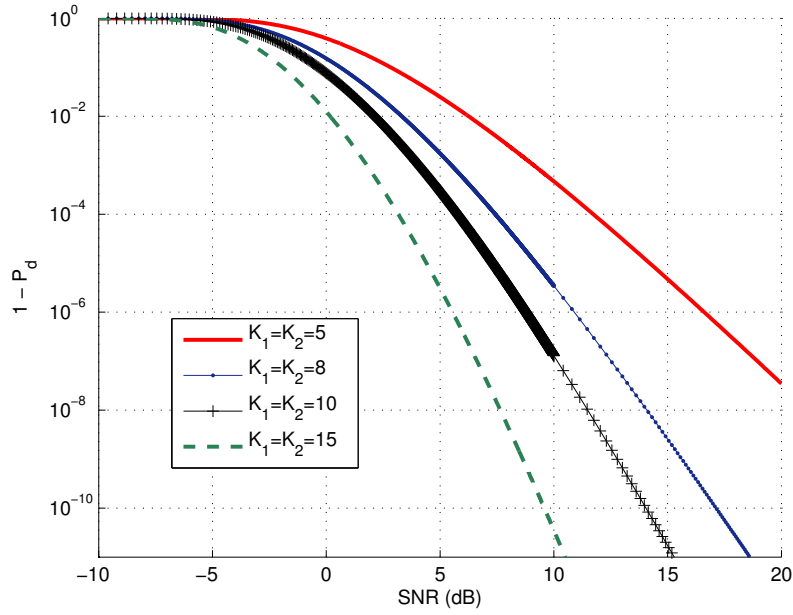


Figure 5.4: The error performance vs. the SNR for varying values of K_1 and K_2 ; $S_1 = 5$, and $S_2 = 0$

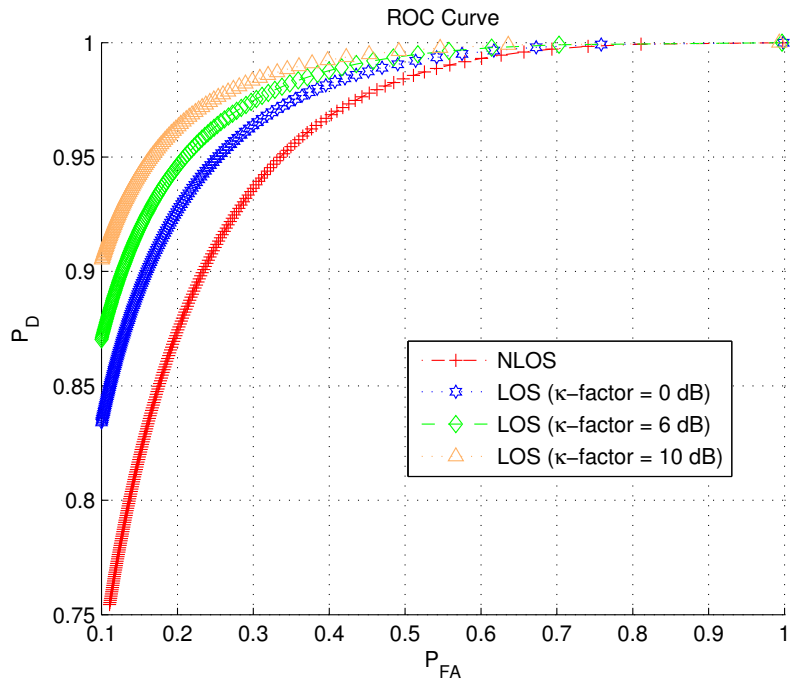


Figure 5.5: The ROC curves for both LOS and NLOS channels at $K_1 = 20$, $K_2 = 10$, and $S_1 = S_2 = 200$.

5.2 Results for Polling of Sensors in a Multi-hop M2M Network

This section presents the comparison of both the analytical and the simulation results for different system parameters of the multi-hop case. The monte-carlo simulations are performed for 100,000 trials. Throughout this section, we consider the fixed value of $\tau = 0.5$, $N = 1$, and $S = 4$.

In Fig. 5.6, the state probability of the packet state $Y(l) = \{1100\}$ is determined against the different number of hops for various values of the transmit power, P , of the OFDM packet. It can be seen that the analytical curves of the state probabilities for the Markov chain are in close approximation to that of the simulation values. Moreover, the results state that the state probability decreases as the hop distance starts to increase between the source and the destination. Moreover, for increasing values of transmit power, P_t , the state probability also increases.

Fig. 5.7 investigates the probability of detection of both the schedules 1 and 2 against different values of transmit power, P for $S = 4$. All the three proposed approaches are compared here for different number of sub-carriers per schedule, K . We assume that the destination node is located 30 hops from the source node. The nodes that follow schedule 1 and 2 are 10 and 20 hops away from the source node, respectively, i.e., $n_1 = n_2 = n_3 = 10$ and $m = 30$. The results here show that for the lenient and diversity approach, the probability of detecting both the schedules at the destination node increases when we increase the number of sub-carriers, K , assigned to each schedule, s . The reason is that, for the lenient case, when K increases,

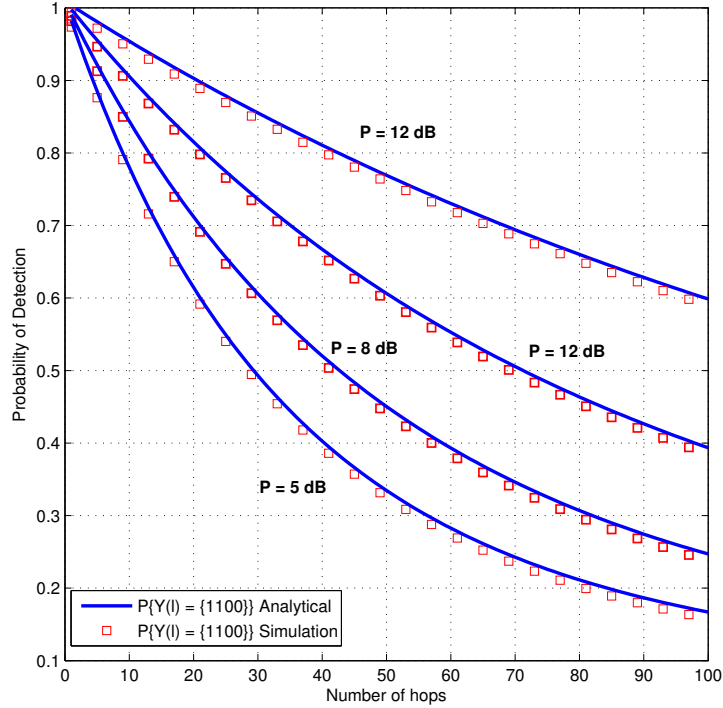


Figure 5.6: The probability of detection for different number of hops for varying P .

the probability of successfully detecting any one sub-carrier out of K sub-carriers increases. For the strict approach, the inverse happens, i.e., when K increases, the probability of successful detection of all the sub-carriers at a time, decreases. It can be observed that the diversity approach is better in terms of detection probability because of the additive effect of K diversity channels. A special case arises for $K = 1$, where all the approaches provide the same performance.

In Fig. 5.8, for the diversity case, the outage probability of both the schedules 1 and 2 is determined for different number of schedules, S , present in a network against various transmit powers. The total number of sub-

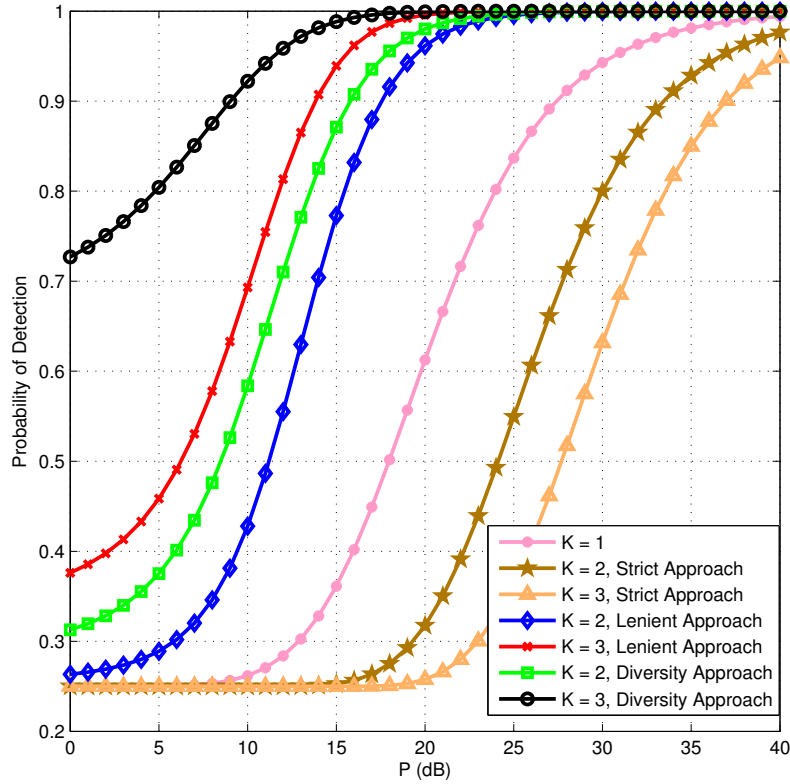


Figure 5.7: The probability of detection against the transmit power, P , for varying K .

carriers, K , assigned per schedule are 3 and the values of n_1 , n_2 and n_3 are assumed to be 10, ie., $n_1 = n_2 = n_3 = 10$. We can observe here that the outage probability increases as the value of S increases. This is due to the fact, that the transmit power of each sub-carrier decreases when we increase the number of schedules in a network. When the value of S increases, the bands in an OFDM packet also increase in order to cater every schedule. Therefore, the total power of an OFDM packet divides by the term KS , and hence each sub-carrier gets a fraction of $1/KS$ of the total OFDM packet

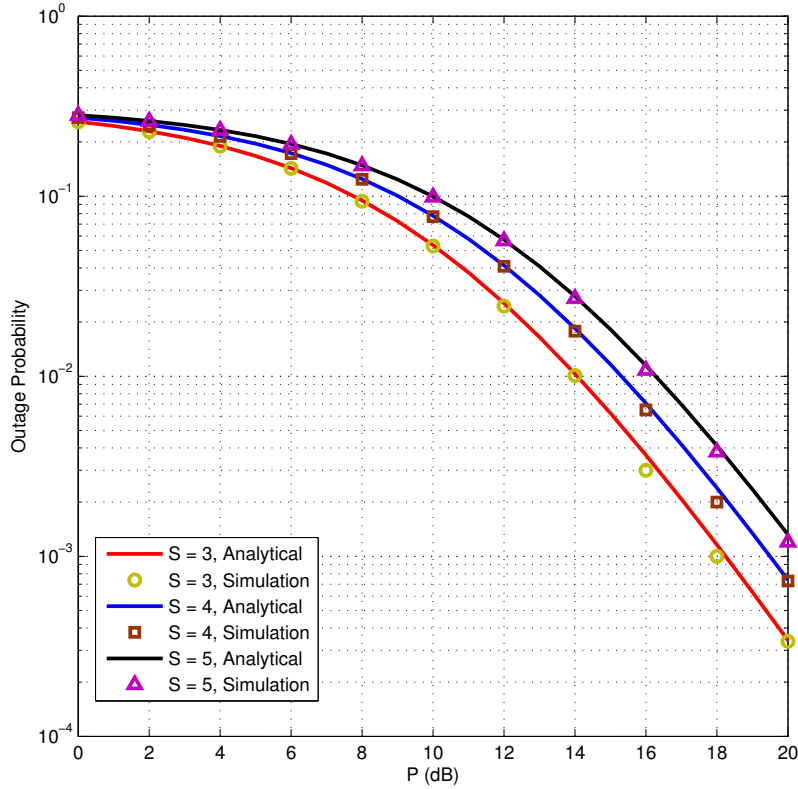


Figure 5.8: The outage probability vs. the transmit power, P , for varying S . power. The analytical results here are also verified by the simulation results.

The probability of detection for different hop combinations, i.e., for different values of n_1 , n_2 and n_3 are investigated in Fig. 5.9 for the diversity scenario. The results are derived by keeping the same source-destination distance for all the combinations, i.e., for $m = 30$. The total schedules, S , and the sub-carriers per schedules, K , are considered to be 4 and 3, respectively. The total transmit power, P , of the OFDM packet is taken as 10dB. For every combination of n_1 , n_2 and n_3 , the gray and blue bars indicate the probability

of detection of schedules 1 and 2, respectively, while, the red and pink bars give the measure of false alarm for the schedules 3 and 4, respectively, in Fig. 5.9. It is shown that, in all the cases, the probability of detection of schedule 2 is higher than that of schedule 1. This is because, the node that follows schedule 2 is somehow closer to the destination as compared to the node that follows schedule 1. This difference in probability increases as the node following schedule 2 moves more closer to the destination. The difference is least for the case when both the nodes are more closer to each other. Also, because of the channel conditions, the schedules 3 and 4, which are not part of the source-destination route also detect at the destination with same probability of false alarm.

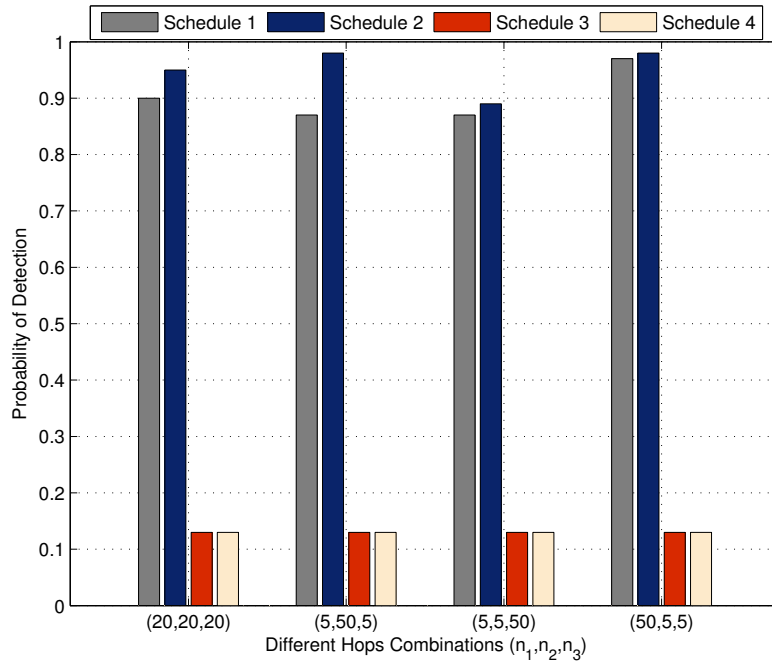


Figure 5.9: The probability of detection for different combinations of n_1 , n_2 and n_3 .

Finally, in Fig. 5.10, the combined outage probability of schedules 1 and 2 and the probability of false alarm of schedules 3 and 4 is determined for varying values of threshold, τ . The curves indicate that as the threshold increases, both the outage probability and the probability of false alarm increases. This is because, the probability of incorrect detection of the schedules increases with increasing value of τ .

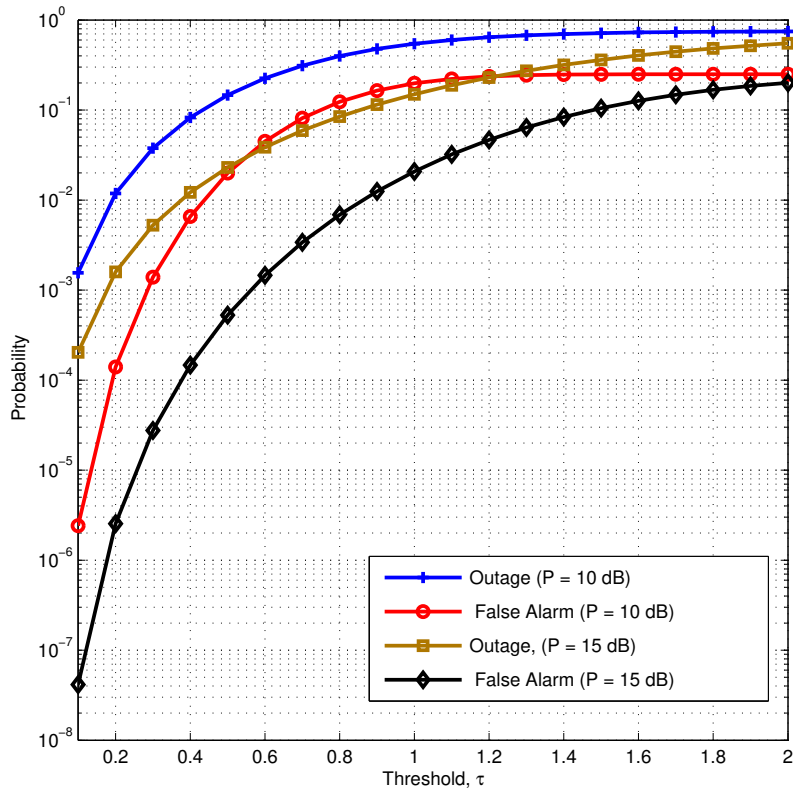


Figure 5.10: The outage probability against different thresholds for $S = 4$.

Chapter 6

Conclusion & Future Works

This chapter concludes the work done in this thesis and also highlights the work in this domain that will be carried out in the near future.

We explored the role of diversity in a one-shot polling scheme in Chapter 3, given certain numbers of sensors reporting detections and non-detections, respectively. A Neyman-Pearson test has been derived assuming independent fading diversity channels with or without the line-of-sight. For example, the technique could be implemented with OFDM and could be used to reduce the latency and overhead when polling a collection of sensors. Diversity order has been shown to play a strong role, enhancing the probability of detecting the signals sent by the sensors.

Chapter 4 investigates three different approaches for finding the schedules in a linear striped-shaped horizontal network. The analytical expressions for each case is derived using the Markov chain model for the irreducible state space in discrete time. For detection of schedules in the network, an OFDM packet is considered that travels all the way to the destination. The inter-

mediate nodes perform energy detection and insert the information of their own schedule, that they follow, in their respective sub-carriers. The destination, when detects the schedules that are occupied in the network, provides the source node with a different schedule that is not already in use, for data transmission.

Ideas for future work include the following suggestions:

- The practical implementation of the OFDMA systems in order to evaluate the more realistic readings.
- The prior probabilities of the sensor nodes will be catered for the future studies.
- In the single-hop analysis, the multiple-hypothesis testing will be performed in order to detect multiple decisions of the sensor nodes.
- The work done on a single striped-shape network will be generalized for the case of n hops in a level.

Bibliography

- [1] B. Mostefa and G. Abdelkader, “A survey of wireless sensor network security in the context of internet of things,” in *2017 4th International Conference on Information and Communication Technologies for Disaster Management (ICT-DM)*, Dec 2017, pp. 1–8.
- [2] Z. Chu, F. Zhou, Z. Zhu, R. Q. Hu, and P. Xiao, “Wireless powered sensor networks for internet of things: Maximum throughput and optimal power allocation,” *IEEE Internet of Things Journal*, vol. 5, no. 1, pp. 310–321, Feb 2018.
- [3] R. Al-Zaidi, J. C. Woods, M. Al-Khalidi, and H. Hu, “Building novel vhf-based wireless sensor networks for the internet of marine things,” *IEEE Sensors Journal*, vol. 18, no. 5, pp. 2131–2144, March 2018.
- [4] D. Sharma and A. P. Bhondekar, “Traffic and energy aware routing for heterogeneous wireless sensor networks,” *IEEE Communications Letters*, pp. 1–1, 2018.
- [5] H. Li and A. V. Savkin, “Wireless sensor network based navigation of micro flying robots in the industrial internet of things,” *IEEE Transactions on Industrial Informatics*, pp. 1–1, 2018.

- [6] E. M. Royer and C.-K. Toh, "A review of current routing protocols for ad hoc mobile wireless networks," *IEEE Personal Communications*, vol. 6, no. 2, pp. 46–55, Apr 1999.
- [7] L. A. Latiff and N. Fisal, "Routing protocols in wireless mobile ad hoc network - a review," in *9th Asia-Pacific Conference on Communications (IEEE Cat. No.03EX732)*, vol. 2, Sept 2003, pp. 600–604 Vol.2.
- [8] H. A. Mogaibel and M. Othman, "Review of routing protocols and it's metrics for wireless mesh networks," in *2009 International Association of Computer Science and Information Technology - Spring Conference*, April 2009, pp. 62–70.
- [9] A. Scaglione and Y.-W. Hong, "Opportunistic large arrays: cooperative transmission in wireless multihop ad hoc networks to reach far distances," *IEEE Transactions on Signal Processing*, vol. 51, no. 8, pp. 2082–2092, Aug 2003.
- [10] S. Biradar and P. Kulkarni, "Enhancing the quality of service using m-aodv protocol in manets," in *2015 International Conference on Applied and Theoretical Computing and Communication Technology (iCATccT)*, Oct 2015, pp. 648–652.
- [11] S. D. Ibrahim, O. C. Ugweje, A. M. Aibinu, G. Koyunlu, and S. Adeshina, "Performance of wireless body area network in the presence of multipath and fading," in *2017 13th International Conference on Electronics, Computer and Computation (ICECCO)*, Nov 2017, pp. 1–6.

- [12] A. Dhaka, V. Bhaskar, A. Nandal, and N. Marina, “Statistical approach using phase variance for analysing correlated multipath fading environment,” *IET Communications*, vol. 12, no. 8, pp. 948–955, 2018.
- [13] J. A. Anastasov, Z. M. Marjanovic, D. N. Milic, and G. T. Djordjevic, “Average ber and noisy reference loss of partially coherent psk demodulation over shadowed multipath fading channel,” *IEEE Transactions on Vehicular Technology*, pp. 1–1, 2018.
- [14] W. H. Tranter, D. P. Taylor, R. E. Ziemer, N. F. Maxemchuk, and J. W. Mark, *A Simple Transmit Diversity Technique for Wireless Communications*. Wiley-IEEE Press, 2007, pp. 692–. [Online]. Available: <https://ieeexplore.ieee.org/xpl/articleDetails.jsp?arnumber=5273250>
- [15] A. Sendonaris, E. Erkip, and B. Aazhang, “Increasing uplink capacity via user cooperation diversity,” in *Proceedings. 1998 IEEE International Symposium on Information Theory (Cat. No.98CH36252)*, Aug 1998, pp. 156–.
- [16] J. N. Laneman, G. W. Wornell, and D. N. C. Tse, “An efficient protocol for realizing cooperative diversity in wireless networks,” in *Proceedings. 2001 IEEE International Symposium on Information Theory (IEEE Cat. No.01CH37252)*, 2001, pp. 294–.
- [17] A. Kailas, L. Thanayankizil, and M. A. Ingram, “A simple cooperative transmission protocol for energy-efficient broadcasting over multi-hop wireless networks,” *Journal of Communications and Networks*, vol. 10, no. 2, pp. 213–220, June 2008.

- [18] S. A. Hassan and M. A. Ingram, "Analysis of an opportunistic large array line network with bernoulli node deployment," *IET Communications*, vol. 8, no. 1, pp. 19–26, Jan 2014.
- [19] H. Jung and M. A. Weitnauer, "Multi-packet opportunistic large array transmission on strip-shaped cooperative routes or networks," *IEEE Transactions on Wireless Communications*, vol. 13, no. 1, pp. 144–158, January 2014.
- [20] V. Rohokale, N. Kulkarni, N. Prasad, and H. Cornean, "Cooperative opportunistic large array approach for cognitive radio networks," in *2010 8th International Conference on Communications*, June 2010, pp. 513–516.
- [21] Y.-W. Hong and A. Scaglione, "Cooperative transmission in wireless multi-hop ad hoc networks using opportunistic large arrays (ola)," in *2003 4th IEEE Workshop on Signal Processing Advances in Wireless Communications - SPAWC 2003 (IEEE Cat. No.03EX689)*, June 2003, pp. 120–124.
- [22] L. Thanayankizil and M. A. Ingram, "Reactive robust routing with opportunistic large arrays," in *2009 IEEE International Conference on Communications Workshops*, June 2009, pp. 1–5.
- [23] L. V. Thanayankizil, A. Kailas, and M. A. Ingram, "Two energy-saving schemes for cooperative transmission with opportunistic large arrays," in *IEEE GLOBECOM 2007 - IEEE Global Telecommunications Conference*, Nov 2007, pp. 1038–1042.

- [24] H. Luo, K. Wu, R. Ruby, Y. Liang, Z. Guo, and L. M. Ni, “Software-defined architectures and technologies for underwater wireless sensor networks: A survey,” *IEEE Communications Surveys Tutorials*, pp. 1–1, 2018.
- [25] D. Sharma and A. P. Bhondekar, “Traffic and energy aware routing for heterogeneous wireless sensor networks,” *IEEE Communications Letters*, pp. 1–1, 2018.
- [26] E. Ortega, G. Aranguren, M. J. Senz, R. Gutierrez, and J. C. Jimeno, “Wireless sensor network for photovoltaic modules monitoring,” in *2017 IEEE 44th Photovoltaic Specialist Conference (PVSC)*, June 2017, pp. 1–5.
- [27] K. Muthukumaran, K. Chitra, and C. Selvakumar, “Energy efficient clustering in wireless sensor networks,” in *2017 International Conference on Inventive Computing and Informatics (ICICI)*, Nov 2017, pp. 351–355.
- [28] J. B. Hughes, P. Lazaridis, I. Glover, and A. Ball, “An empirical study of link quality assessment in wireless sensor networks applicable to transmission power control protocols,” in *Loughborough Antennas Propagation Conference (LAPC 2017)*, Nov 2017, pp. 1–5.
- [29] M. Baghaie and B. Krishnamachari, “Fast flooding using cooperative transmissions in wireless networks,” in *2009 IEEE International Conference on Communications*, June 2009, pp. 1–5.

- [30] A. Aksu and O. Ercetin, "Multi-hop cooperative transmissions in wireless sensor networks," in *2006 2nd IEEE Workshop on Wireless Mesh Networks*, Sept 2006, pp. 132–134.
- [31] X. Li, M. Chen, and W. Liu, "Cooperative transmissions in wireless sensor networks with imperfect synchronization," in *Conference Record of the Thirty-Eighth Asilomar Conference on Signals, Systems and Computers, 2004.*, vol. 1, Nov 2004, pp. 1281–1285 Vol.1.
- [32] C. Zhang, J. Ge, Z. Xia, and H. Du, "Graph theory based cooperative transmission for physical-layer security in 5g large-scale wireless relay networks," *IEEE Access*, vol. 5, pp. 21 640–21 649, 2017.
- [33] N. Atitallah, H. Hakim, K. Loukil, A. M. Obeid, and M. Abid, "Energy efficient adaptive transmission strategy using cooperative diversity for wireless sensor networks," in *2016 IEEE 27th Annual International Symposium on Personal, Indoor, and Mobile Radio Communications (PIMRC)*, Sept 2016, pp. 1–6.
- [34] I. Zahiri, J. Hamedoun, H. Bouzekri, and G. Aniba, "Cooperative wireless transmission for smart metering," in *2016 IEEE International Conference on Smart Grid Communications (SmartGridComm)*, Nov 2016, pp. 249–253.
- [35] J. N. Laneman and G. W. Wornell, "Distributed space-time-coded protocols for exploiting cooperative diversity in wireless networks," *IEEE Transactions on Information Theory*, vol. 49, no. 10, pp. 2415–2425, Oct 2003.

- [36] M. Vajapeyam and U. Mitra, "Performance analysis of distributed space-time coded protocols for wireless multi-hop communications," *IEEE Transactions on Wireless Communications*, vol. 9, no. 1, pp. 122–133, January 2010.
- [37] S. A. Hassan and M. A. Ingram, "The benefit of co-locating groups of nodes in cooperative line networks," *IEEE Communications Letters*, vol. 16, no. 2, pp. 234–237, February 2012.
- [38] S. A. Hasan and M. A. Ingram, "A quasi-stationary markov chain model of a cooperative multi-hop linear network," *IEEE Transactions on Wireless Communications*, vol. 10, no. 7, pp. 2306–2315, July 2011.
- [39] M. Bacha and S. A. Hassan, "Performance analysis of linear cooperative multi-hop networks subject to composite shadowing-fading," *IEEE Transactions on Wireless Communications*, vol. 12, no. 11, pp. 5850–5858, November 2013.
- [40] S. A. Hassan, "Performance analysis of cooperative multi-hop strip networks," *Wireless Personal Communications*, vol. 74, no. 2, pp. 391–400, Jan 2014. [Online]. Available: <https://doi.org/10.1007/s11277-013-1291-9>
- [41] S. A. Hassan and M. A. Ingram, "Analysis of an opportunistic large array line network with bernoulli node deployment," *IET Communications*, vol. 8, no. 1, pp. 19–26, Jan 2014.

- [42] A. Afzal and S. A. Hassan, "Stochastic modeling of cooperative multi-hop strip networks with fixed hop boundaries," *IEEE Transactions on Wireless Communications*, vol. 13, no. 8, pp. 4146–4155, Aug 2014.
- [43] M. Hussain and S. A. Hassan, "Performance of multi-hop cooperative networks subject to timing synchronization errors," *IEEE Transactions on Communications*, vol. 63, no. 3, pp. 655–666, March 2015.
- [44] M. Ahsen, S. A. Hassan, and D. N. K. Jayakody, "Propagation modeling in large-scale cooperative multi-hop ad hoc networks," *IEEE Access*, vol. 4, pp. 8925–8937, 2016.
- [45] M. Hussain and S. A. Hassan, "Impact of intra-flow interference on the performance of 2-d multi-hop cooperative network," *IEEE Communications Letters*, vol. 21, no. 4, pp. 869–872, April 2017.
- [46] M. A. Aslam and S. A. Hassan, "Analysis of linear network coding in cooperative multi-hop networks," *Wireless Personal Communications*, vol. 95, no. 4, pp. 4967–4981, Aug 2017. [Online]. Available: <https://doi.org/10.1007/s11277-017-4141-3>
- [47] M. S. Bahbahani and E. Alsusa, "Dc-leach: A duty-cycle based clustering protocol for energy harvesting wsns," in *2017 13th International Wireless Communications and Mobile Computing Conference (IWCMC)*, June 2017, pp. 974–979.
- [48] V. Kumar and S. Tiwari, "Performance of routing protocols for beacon-enabled ieee 802.15.4 wsns with different duty cycle," in *2011 Inter-*

- national Conference on Devices and Communications (ICDeCom)*, Feb 2011, pp. 1–5.
- [49] J. Li, D. Zhang, L. Guo, S. Ji, and Y. Li, “M-cube: A duty cycle based multi-channel mac protocol with multiple channel reservation for wsns,” in *2010 IEEE 16th International Conference on Parallel and Distributed Systems*, Dec 2010, pp. 107–114.
- [50] D. Ghose, F. Y. Li, and V. Pla, “Mac protocols for wake-up radio: Principles, modeling and performance analysis,” *IEEE Transactions on Industrial Informatics*, vol. 14, no. 5, pp. 2294–2306, May 2018.
- [51] S. Argoubi, K. Maalaoui, M. H. Elhdhili, and L. A. Saidane, “Priority-mac: A priority based medium access control solution with qos for wsn,” in *2016 IEEE/ACS 13th International Conference of Computer Systems and Applications (AICCSA)*, Nov 2016, pp. 1–6.
- [52] R. Munadi, A. E. Sulistyorini, F. U. F. S, and T. Adiprabowo, “Simulation and analysis of energy consumption for s-mac and t-mac protocols on wireless sensor network,” in *2015 IEEE Asia Pacific Conference on Wireless and Mobile (APWiMob)*, Aug 2015, pp. 142–146.
- [53] E. Aghayi, M. Khansari, and H. Memarzadeh-Tehran, “A new back-off mechanism for the s-mac protocol with applications in healthcare,” in *Telecommunications (IST), 2014 7th International Symposium on*, Sept 2014, pp. 569–573.
- [54] E. Kaljic and S. Konjicija, “Multi-objective parameter optimization of s-mac protocol,” in *2014 37th International Convention on Informa-*

- tion and Communication Technology, Electronics and Microelectronics (MIPRO)*, May 2014, pp. 545–550.
- [55] A. N. A. Pantazis, A. Pantazis, S. A. Nikolidakis, and D. D. Vergados, “A performance evaluation of s-mac protocol in combination with energy efficient protocols for wireless sensor networks,” in *2011 18th International Conference on Telecommunications*, May 2011, pp. 186–190.
- [56] F. Hamady, M. Sabra, Z. Sabra, A. Kayssi, A. Chehab, and M. Mansour, “Enhancement of the s-mac protocol for wireless sensor networks,” in *2010 International Conference on Energy Aware Computing*, Dec 2010, pp. 1–4.
- [57] J. Han, P. K. Varshney, and R. Srinivasan, “Distributed binary integration,” *IEEE Transactions on Aerospace and Electronic Systems*, vol. 29, no. 1, pp. 2–8, Jan 1993.
- [58] F. Gini, F. Lombardini, and L. Verrazzani, “Decentralized cfar detection with binary integration in weibull clutter,” *IEEE Transactions on Aerospace and Electronic Systems*, vol. 33, no. 2, pp. 396–407, April 1997.
- [59] R. S. Blum and B. M. Sadler, “Energy efficient signal detection in sensor networks using ordered transmissions,” *IEEE Transactions on Signal Processing*, vol. 56, no. 7, pp. 3229–3235, July 2008.
- [60] P. Braca, S. Marano, and V. Matta, “Single-transmission distributed detection via order statistics,” *IEEE Transactions on Signal Processing*, vol. 60, no. 4, pp. 2042–2048, April 2012.

- [61] I. C. Paschalidis, F. Huang, and W. Lai, "Distributed scheduling of wireless networks: A message passing approach," in *21st Mediterranean Conference on Control and Automation*, June 2013, pp. 922–929.
- [62] B. W. Cook, S. Lanzisera, and K. S. J. Pister, "Soc issues for rf smart dust," *Proceedings of the IEEE*, vol. 94, no. 6, pp. 1177–1196, June 2006.
- [63] P. S. Rossi, D. Ciuonzo, and G. Romano, "Orthogonality and cooperation in collaborative spectrum sensing through mimo decision fusion," *IEEE Transactions on Wireless Communications*, vol. 12, no. 11, pp. 5826–5836, November 2013.
- [64] D. Ciuonzo, A. D. Maio, and P. S. Rossi, "A systematic framework for composite hypothesis testing of independent bernoulli trials," *IEEE Signal Processing Letters*, vol. 22, no. 9, pp. 1249–1253, Sept 2015.
- [65] T. He and L. Tong, "Detection of information flows," *IEEE Transactions on Information Theory*, vol. 54, no. 11, pp. 4925–4945, Nov 2008.
- [66] T. H and L. Tong, "Distributed detection of information flows," *IEEE Transactions on Information Forensics and Security*, vol. 3, no. 3, pp. 390–403, Sept 2008.
- [67] T. Ali-Yahiya, A. L. Beylot, and G. Pujolle, "Channel aware scheduling for multiple service flows in ofdma based mobile wimax systems," in *2008 IEEE 68th Vehicular Technology Conference*, Sept 2008, pp. 1–5.
- [68] A. Akanser and M. A. Ingram, "Semi-cooperative spectrum fusion (scsf) for aerial reading of a correlated sensor field," in *2009 1st International*

Conference on Wireless Communication, Vehicular Technology, Information Theory and Aerospace Electronic Systems Technology, May 2009, pp. 732–736.

- [69] A. Castaño-Martínez and F. López-Blázquez, “Distribution of a sum of weighted noncentral chi-square variables,” *TEST*, vol. 14, no. 2, pp. 397–415, Dec 2005. [Online]. Available: <https://doi.org/10.1007/BF02595410>
- [70] M. Ahsen, S. A. Hassan, and D. N. K. Jayakody, “Propagation modeling in large-scale cooperative multi-hop ad hoc networks,” *IEEE Access*, vol. 4, pp. 8925–8937, Dec 2016.
- [71] M. Simon, *Probability Distributions Involving Gaussian Random Variables: A Handbook for Engineers and Scientists*. Springer US, 2006.
- [72] F. J. Massey, “The kolmogorov-smirnov test for goodness of fit,” *Journal of the American Statistical Association*, vol. 46, no. 253, pp. 68–78, 1951. [Online]. Available: <http://www.jstor.org/stable/2280095>
- [73] E. Senta, *Non-Negative Matrices and Markov Chains*, 2nd ed. Springer US, 2006.
- [74] S. M. Ross, *Introduction to Probability Models*, 9th ed. Academic Press, 2007.